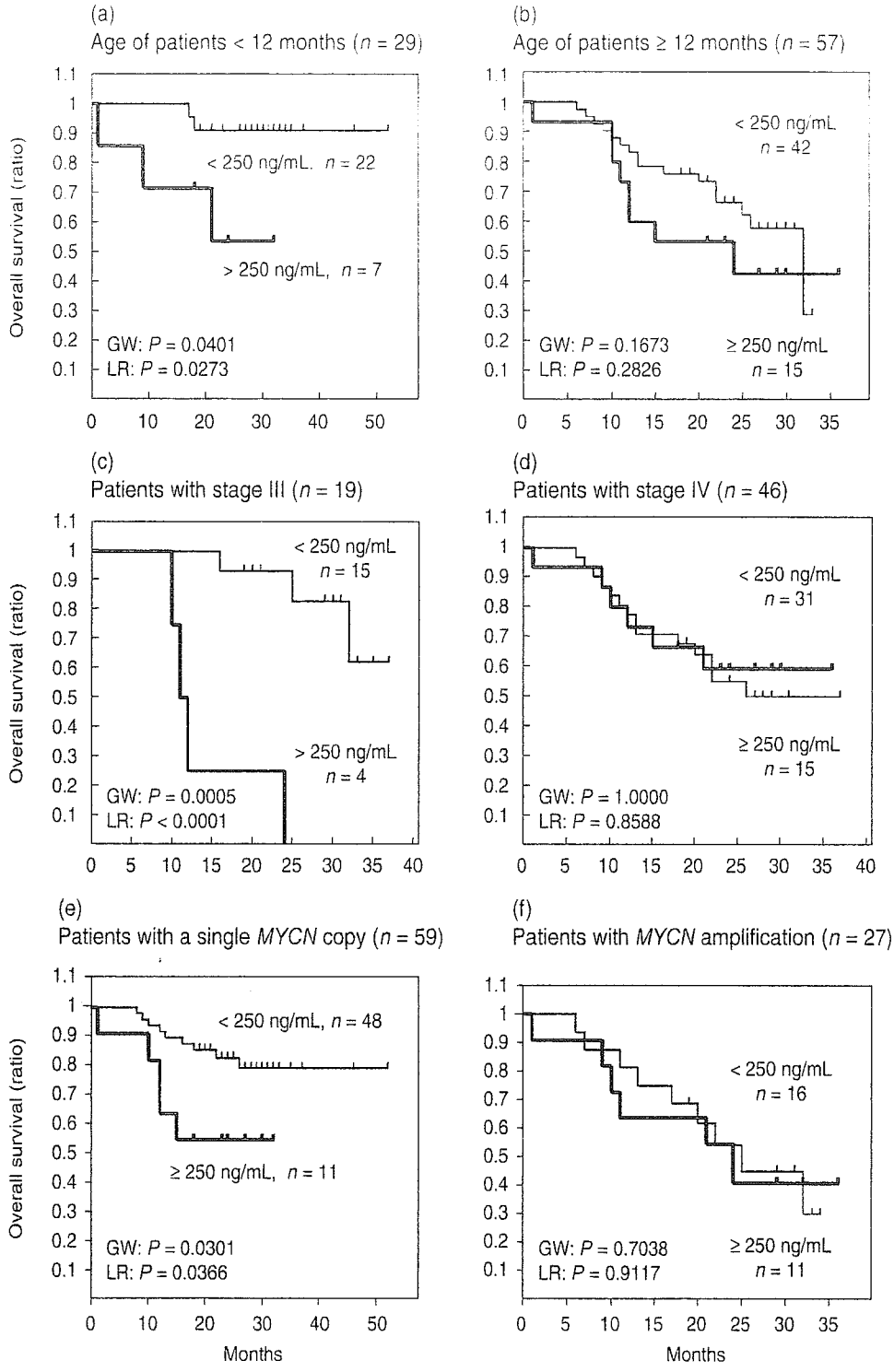

Fig. 3. Clinical significance of the serum NM23-H1 levels in the groups classified according to the age of the patients, or stage of the disease, or copy number of *MYCN*. (a) Survival curves for seven patients with a serum NM23-H1 level of ≥ 250 ng/mL, and for 22 patients with a level < 250 ng/mL. Both groups of patients were younger than 12 months of age. (b) Survival curves for 15 patients with a serum NM23-H1 level of ≥ 250 ng/mL, and for 42 patients with a level < 250 ng/mL. Both groups of patients were 12 months old or older. (c) Survival curves for four patients with a serum NM23-H1 level of ≥ 250 ng/mL, and for 15 patients with a level < 250 ng/mL. Both groups of patients were at stage 3 of the disease. (d) Survival curves for 15 patients with the serum NM23-H1 level ≥ 250 ng/mL, and for 31 patients with the level < 250 ng/mL. Both groups of patients were at stage 4 of the disease. (e) Survival curves for 11 patients with a serum NM23-H1 level of ≥ 250 ng/mL, and for 48 patients with a level < 250 ng/mL. Both groups of patients had a single copy of *MYCN*. (f) Survival curves for 11 patients with a serum NM23-H1 level of ≥ 250 ng/mL, and for 16 patients with a level < 250 ng/mL. Both groups of patients had *MYCN* amplification in the tumor. GW, generalized Wilcoxon's test; LR, log-rank test.

 doi: 10.1111/j.1349-7006.2005.00091.x

and serum NSE is a useful marker for patients with advanced neuroblastoma in whom the elevated levels are associated with a poor outcome.[27] The disialoganglioside GD2 is found on the surface of most neuroblastoma cells, and elevated plasma levels have been found in patients.[28] Nevertheless, none of these markers is used at present to predict clinical outcomes or to choose treatment protocols. Therefore, serum NM23-H1 levels might be useful for clinical purposes.

The elevated serum level of NM23-H1 was correlated with a poor prognostic feature, namely, *MYCN* amplification (Table 1). Godfrid *et al.* identified genes that are part of the *MYCN* downstream pathway using SAGE libraries of *MYCN* transfected and control neuroblastoma cell lines.[13] The chromosome 17q genes *NM23-H1* and *NM23-H2* were strongly induced in *MYCN*-expressing cells. A striking correlation between *MYCN* amplification and mRNA or protein expression of both *NM23* genes was found in the cell lines. The present multivariate analysis showed no influence of serum NM23-H1 level on overall survival, and this finding might be caused by the overlap of patients with *MYCN* amplification with those with a high serum level of NM23-H1. However, within the group of patients with a single copy of *MYCN*, patients with a higher level of NM23-H1 had a worse outcome (Fig. 3e). The findings suggest that *NYCN* amplification may influence serum NM23-H1 levels as well as clinical outcome, and that neuroblastomas with a single copy of *MYCN* and a higher serum NM23-H1 level may have had a mutation or an increased copy number of the *NM23-H1* gene.[6,24,29] *MYCN* overexpression in some neuroblastomas with a single copy of *MYCN* may have resulted in higher serum NM23-H1 levels and a poor outcome; however, a recent study showed that *MYCN* overexpression did not affect the prognosis of advanced-stage neuroblastomas with a single *MYCN* copy.[30]

In patients with NHL and AML, it is thought that serum NM23-H1 protein is produced directly by the tumor cells, and its serum level depends on the total mass of malignant cells overexpressing *NM23-H1*.[14] High concentrations of NM23 protein were found in the serum and body fluid of patients with lung cancer overexpressing the *NM23* genes.[31] Tumor cells may secrete this protein through some unknown mechanism, because there is no signal peptide sequence for secretion in the NM23 molecule. Serum NM23-H1 in patients with neuroblastoma might be derived from tumor cells and might be induced by *MYCN* amplification/overexpression or by *NM23-H1* overexpression independent of *MYCN*.

The serum level of NM23-H1 protein is clinically useful as an important prognostic factor in NHL or AML, and the present study showed that the protein could be a factor predicting an outcome of patients with neuroblastoma. It would be interesting to examine whether the serum NM23-H1 level generally predicts a poor outcome for patients with other tumors. The mechanisms by which the NM23-H1 protein is secreted into the serum and how it affects patient outcome are unclear. We are now studying the possibility that a high concentration of serum NM23-H1 may positively affect tumor cell growth or negatively affect normal cells.

Acknowledgments

We thank Ms K. Yagyu for secretarial assistance. We also appreciate the help of a number of physicians who provided clinical data, and the patients and control children who donated blood. This study was supported in part by Grants-in-Aid from the Ministry of Education, Culture, Sports, Science and Technology, and the Ministry of Health, Labor and Welfare of Japan for the Second Term Comprehensive 10-year Strategy for Cancer Control.

References

1 Steeg PS, Bevilacqua G, Kopper L *et al.* Evidence for a novel gene associated with low tumor metastatic potential. *J Natl Cancer Inst* 1988; **80**: 200–4.
2 Lacombe ML, Milon L, Munier A, Mehus JG, Lambeth DO. The human nm23/nucleoside diphosphate kinases. *J Bioenerg Biomembr* 2000; **32**: 247–58.
3 Lascu I, Gonin P. The catalytic mechanism of nucleoside diphosphate kinases. *J Bioenerg Biomembr* 2000; **32**: 237–46.
4 MacDonald NJ, Rosa ADL, Steeg PS. The potential roles of nm23 in cancer metastasis and cellular differentiation. *Eur J Cancer* 1995; **31A**: 1096–100.
5 Lacombe ML, Sastre-Garau X, Lascu I *et al.* Overexpression of nucleoside diphosphate kinase (Nm23) in solid tumors. *Eur J Cancer* 1991; **27**: 1302–7.
6 Leone A, Seeger RC, Hong CM *et al.* Evidence for nm23 RNA overexpression, DNA amplification and mutation in aggressive childhood neuroblastoma. *Oncogene* 1993; **8**: 855–65.
7 Chang C, Zhu X-X, Thoraval D *et al.* nm23–H1 mutation in neuroblastoma. *Nature (London)* 1994; **370**: 335–6.
8 Yokoyama A, Okabe-Kado J, Wakimoto N *et al.* Evaluation by multivariate analysis of the differentiation inhibitory factor nm23 as a prognostic factor in acute myelogenous leukemia and application to other hematological malignancies. *Blood* 1998; **91**: 1845–51.
9 Hailat N, Keim DR, Melhem RF *et al.* High levels of p19/nm23 protein in neuroblastoma are associated with advanced stage disease and with N-myc gene amplification. *J Clin Invest* 1991; **88**: 341–5.
10 Niitsu N, Okabe-Kado J, Okamoto M *et al.* Serum nm23-H1 protein as a prognostic factor in aggressive non-Hodgkin's lymphoma. *Blood* 2001; **97**: 1202–10.
11 Bown N, Cotterill S, Lastowska M *et al.* Gain of chromosome arm 17q and adverse outcome in patients with neuroblastoma. *N Engl J Med* 1999; **340**: 1954–61.
12 Kaneko Y, Kobayashi H, Maseki N, Nakagawara A, Sakurai M. Disomy 1 with terminal 1p deletion was frequent in mass screening-negative/late-presenting neuroblastomas in young children, but not in mass screening-positive neuroblastomas in infants. *Int J Cancer* 1999; **80**: 54–9.
13 Godfried MB, Veenstra MV, Sluis P *et al.* The N-myc and c-myc downstream pathways include the chromosome 17q genes nm23-H1 and nm23-H2. *Oncogene* 2002; **21**: 2097–101.
14 Okabe-Kado J. Serum nm23-H1 protein as a prognostic factor in hematological malignancies. *Leuk Lymphoma* 2002; **43**: 859–67.
15 Niitsu N, Okabe-Kado J, Nakayama M *et al.* Plasma levels of the differentiation inhibitory factor nm23-H1 protein and their clinical implication in acute myelogenous leukemia. *Blood* 2000; **96**: 1080–6.
16 Niitsu N, Nakamine H, Okamoto M *et al.* Clinical significance of intracytoplasmic nm23-H1 expression in diffuse large B-cell lymphoma. *Clin Cancer Res* 2004; **10**: 2482–90.
17 Sawada T, Hirayama M, Nakata T *et al.* Mass screening for neuroblastoma in infants in Japan. *Lancet* 1984; **2**: 271–3.
18 Brodeur GM, Pritchard J, Berthold F *et al.* Revision of the international criteria for neuroblastoma diagnosis, staging, and response to treatment. *J Clinic Oncol* 1993; **11**: 1466–77.
19 Sawaguchi S, Kaneko M, Uchino J *et al.* Treatment of advanced neuroblastoma with emphasis on intensive induction chemotherapy. *Cancer* 1990; **66**: 1879–87.
20 Testa U, Thomopouls P, Vinci G *et al.* Transferrin binding to K562 cell line. *Exp Cell Res* 1982; **140**: 251–60.
21 Bowman LC, Castleberry RP, Cantor A *et al.* Genetic staging of unresectable or metastatic neuroblastoma in infants: a Pediatric Oncology Group Study. *J Nat Cancer Inst* 1997; **89**: 373–80.

22 Nakagawara A, Arima-Nakagawara M, Scavarda NJ, Azar CG, Cantor AB, Brodeua GM. Association between high levels of expression of the *TRK* gene and favorable outcome in human neuroblastoma. *N Engl J Med* 1993; **328**: 847–54
23 Willem R, Van Bockstaele DR, Lardon F *et al*. Decrease in nucleoside diphosphate kinase (NDPK/nm23) expression during hematopoietic maturation. *J Biol Chem* 1998; **273**: 13663–8.
24 Takeda O, Handa M, Uehara T *et al*. An increased NM23-H1 copy number may be a poor prognostic factor independent of LOH on 1p in neuroblastomas. *Br J Cancer* 1996, **74**: 1620–6.
25 Hann H-WL, Evans AE, Siegel SE *et al*. Prognostic importance of serum ferritin in patients with stages III and IV neuroblastoma: The Children's Cancer Study Group Experience. *Cancer Res* 1985; **45**: 2843–8.
26 Shuster JJ, McWilliams NB, Castleberry R *et al*. Serum lactate dehydrogenase in childhood neuroblastoma. A pediatric oncology group recursive partitioning study. *Am J Clin Oncol* 1992; **15**: 295–303.
27 Zeltzer PM, Marangos PJ, Evans AE, Schneider SL. Serum neuron-specific enolase in children with neuroblastoma. Relationship to stage and disease course. *Cancer* 1986; **57**: 1230–4.
28 Landisch S, Wu Z-L. Detection of a tumour-associated ganglioside in plasma of patients with neuroblastoma. *Lancet* 1985; **1**: 136–8.
29 Almgren MAE, Henriksson KCE, Fujimoto J, Chang CL. Nucleoside diphosphate kinase A/nm23-H1 promotes metastasis of NB69-derived human neuroblastoma. *Mol Cancer Res* 2004; **2**: 387–94.
30 Cohn SL, London WB, Huang D *et al*. *MYCN* expression is not prognostic of adverse outcome in advanced-stage neuroblastoma with nonamplified *MYCN*. *J Clin Oncol* 2000; **18**: 3604–13.
31 Huwer H, Kalweit G, Engel M, Welter C, Dooley S, Gams E. Expression of the candidate tumor suppressor gene nm23 in the bronchial system of patients with squamous cell lung cancer. *Eur J Cardiothorac Surg* 1997; **11**: 206–9.

 doi: 10.1111/j.1349-7006.2005.00091.x

VOLUME 23 · NUMBER 22 · AUGUST 1 2005

JOURNAL OF CLINICAL ONCOLOGY

ORIGINAL REPORT

Prediction of *MYCN* Amplification in Neuroblastoma Using Serum DNA and Real-Time Quantitative Polymerase Chain Reaction

Takahiro Gotoh, Hajime Hosoi, Tomoko Iehara, Yasumichi Kuwahara, Shinya Osone, Kunihiko Tsuchiya, Miki Ohira, Akira Nakagawara, Hiroshi Kuroda, and Tohru Sugimoto

From the Department of Pediatrics, Kyoto Prefectural University of Medicine, Graduate School of Medical Science, Kyoto; and Division of Biochemistry, Chiba Cancer Center Research Institute, Chiba, Japan.

Submitted October 6, 2004; accepted April 13, 2005.

Supported by Grants-in-Aid for Scientific Research grant Nos. 15659248, 15659249, and 14370250 from the Ministry of Education, Culture, Sports, Science and Technology of Japan.

Authors' disclosures of potential conflicts of interest are found at the end of this article.

Address reprint requests to Takahiro Gotoh, MD, PhD, Department of Pediatrics, Kyoto Prefectural University of Medicine, Graduate School of Medical Science, Kamigyo-ku, Kyoto 602-8566, Japan; e-mail: takahiro_email@yahoo.co.jp.

0732-183X/05/2322-5205/$20.00

DOI: 10.1200/JCO.2005.02.014

ABSTRACT

Purpose
MYCN amplification (MNA) indicates a poor prognosis in neuroblastoma (NB) and is routinely assayed for therapy stratification. We aimed to develop a diagnostic tool to predict *MYCN* status using serum DNA, which, in cancer patients, predominantly originates from tumor-released DNA.

Patients and Methods
Using DNA-based real-time quantitative polymerase chain reaction, we simultaneously quantified *MYCN* (2p24) and a reference gene, *NAGK* (2p12), and evaluated *MYCN* copy number as an *MYCN/NAGK* (*M/N*) ratio in 87 NB patients whose *MYCN* status had been determined by Southern blotting. Of these patients, 17 had *MYCN*-amplified NB, and 70 had nonamplified NB.

Results
The serum *M/N* ratio in the MNA group (median, 199.32; range, 17.1 to 901.6; 99% CI, 107.0 to 528.7) was significantly ($P < .001$) higher than the ratio in the non-MNA group (median, 0.87; range, 0.25 to 4.6; 99% CI, 0.82 to 1.26; Mann-Whitney *U* test). The sensitivity and specificity of the serum *M/N* ratio as a diagnostic test were both 100% when the serum *M/N* ratio cutoff was set at 10.0. Among six MNA patients whose clinical courses were followed, the serum ratios decreased to the normal range in the patients in remission (n = 3), whereas the ratios increased to high levels in the patients who relapsed (n = 2) or failed to achieve remission (n = 1).

Conclusion
Measurement of the serum *M/N* ratio seems to be a promising method for accurately assessing *MYCN* status in NB, although a larger set of patients needs to be examined to confirm this result.

J Clin Oncol 23:5205-5210. © 2005 by American Society of Clinical Oncology

INTRODUCTION

Neuroblastoma (NB) is the most common extracranial solid tumor in children and is characterized by a wide range of clinical behaviors, from spontaneous regression to rapid progression with a fatal outcome. The clinical heterogeneity has been reported to be associated with a variety of biologic features of NB. One such aberration, *MYCN* amplification (MNA; ie, creation of multiple copies of the *MYCN* gene in the nuclei of tumor cells), is strongly associated with rapid tumor progression and a poor outcome. MNA is detected in 4% of patients in the early stages of NB, 8% of patients in stage 4S, and approximately 30% of patients in advanced stages. Currently, assessment of *MYCN* status is essential for determining therapy stratification in NB.[1-6] Having rapid access to selected biologic data for each tumor has become increasingly important in

routing patients to appropriate therapies. Several years ago, fluorescence in situ hybridization (FISH) replaced Southern blotting as the most accurate and timely way of evaluating tumors for MNA. Using FISH, the turnaround time for results was shortened from weeks to days, making its use in clinical trials realistic.

In this study, we describe a real-time polymerase chain reaction (PCR) method for evaluating *MYCN* status that shortens the turnaround for results to just a few hours. Furthermore, to facilitate the evaluation of *MYCN* status of tumors, we used serum DNA for the PCR template, which, in cancer patients, predominantly consists of tumor-released DNA.[7] Quantification of serum DNA has also been proposed as a screening tool for early detection of lung cancer.[8] Several groups were able to detect tumor-related aberrations, such as loss of heterozygosity and mutations in the *p53* gene, using the serum DNA of patients with a malignant tumor.[9-11]

Recently, Combaret et al[12] reported that high levels of *MYCN* DNA were present in the peripheral blood of patients with *MYCN*-amplified NB. However, they evaluated serum *MYCN* (2p24) dosage based on PCR without a reference gene, so their assay could be influenced by the quality of the template DNA or a numerical change of chromosome 2. To avoid these problems, we used DNA-based real-time quantitative PCR and a single copy reference gene, the *N-acetylglucosamine kinase* gene (*NAGK*; 2p12), so that *MYCN* copy number per chromosome 2 could be evaluated as the *MYCN/NAGK* (*M/N*) ratio. *NAGK* was chosen because it is on the same chromosome as *MYCN* but sufficiently distant from the region spanned by the *MYCN* amplicon (2p12 *v* 2p24)[13] that a numerical change in chromosome 2 would not affect the *M/N* ratio. The diagnostic performance of the test was evaluated in patients with an NB whose *MYCN* status had been determined by Southern blotting.

PATIENTS AND METHODS

Subjects

Eighty-seven patients diagnosed with NB at the Hospital of the Kyoto Prefectural University of Medicine and Chiba Cancer Center Research Institute were enrolled onto this study with the informed consent of their parents. The studies were conducted under research protocols approved by each institutional review board. At the time of diagnosis, 44 patients were younger than 1 year, and 43 were between 1 and 13 years of age. Seventeen of the patients had MNA, and 70 patients did not have MNA, as determined by Southern blotting. According to the International Neuroblastoma Staging System,[4] the 17 children with MNA included one patient each in stage 1 and 2B, two in stage 3, and 13 in stage 4, whereas the 70 children without MNA included 22 in stage 1, 18 in stage 2A and 2B, five in stage 4S, seven in stage 3, and 18 in stage 4.

Twelve of the 17 patients with MNA and 33 of the 70 nonamplified patients were also analyzed by dual-color FISH technique, as previously described,[14] using an *MYCN* probe (pNb101) and a chromosome 2 centromere probe (D2Z). FISH results of these patients were consistent with the Southern blotting results, although three of the patients who were diagnosed as non-MNA by Southern blotting were found to have one to four extra copies of the *MYCN* gene relative to the chromosome 2 centromere number by FISH. This low level of amplification has been defined as *MYCN* gain, which is an intermediate stage between MNA and non-MNA.[15] Because the prognostic significance of *MYCN* gain is still unclear, these patients were classified as non-MNA according to the Southern blotting results.

Sample Preparation

Tumor specimens were surgically resected and immediately stored at −80°C. Peripheral blood was obtained from each patient before any therapy and surgery. To avoid contamination of serum DNA by the DNA from WBCs, we prepared serum exclusively from the liquid fraction of clotted blood after centrifugation at 1,000 × *g* for 10 minutes and stored it at −20°C until DNA extraction.

DNA Isolation

DNA was extracted from tissues and serum samples by using the QIAmp tissue and blood kits (Qiagen, GmbH, Hilden, Germany), respectively, according to the manufacturer's protocols. For each patient, 200 μL of the stored serum was used for extraction of free DNA.

Real-Time Quantitative PCR

TaqMan PCR was performed using the ABI Prism 5700 Sequence Detection System (Applied Biosystems, Foster City, CA). The PCR mixture contained TaqMan universal PCR master mix (Applied Biosystems), 200 nmol/L of each primer, and 100 nmol/L of fluorogenic probe. The principle of the TaqMan analysis has been described previously in detail.[16-18] In addition to the *MYCN* sequence, *NAGK* (GenBank accession No. NM 017567) located at 2p12 was simultaneously measured as a single-copy reference gene. The sequence of primers and the TaqMan probe used for *MYCN* and *NAGK* are as follows: *MYCN* forward, 5′-GTGCTCTCCAATTCTCGCCT-3′; *MYCN* reverse, 5′-GATGGCCTAGAGGAGGGCT-3′; *MYCN* probe, 5′-FAM-CACTAAAGTTCCTTCCACCCTCTCCT-TAMRA-3′; *NAGK* forward, 5′-TGGGCAGACACATCGTAGCA-3′; *NAGK* reverse, 5′-CACCTTCACTCCCACCTCAAC-3′; and *NAGK* probe, 5′-VIC-TGTTGCCCGAGATTGACCCGGT-TAMRA-3′. All PCR reactions were performed with one cycle of 95°C for 5 minutes, followed by PCR amplification with 50 cycles of 95°C for 15 seconds and 60°C for 1 minute. Standard curves were constructed in each PCR run with four-fold serial dilutions containing 20, 5, 1.25, 0.3125, and 0.078125 ng/μL of a healthy donor's DNA in addition to 20 ng/μL of salmon sperm DNA, and the dosages of the target genes in each sample were interpolated using these standard curves. The *MYCN* copy number of a sample of DNA was determined by the ratio of the *MYCN* dosage to the *NAGK* dosage (*M/N* ratio). Copy numbers were expressed as the average of two measurements.

Effect of WBC Contamination

To assess the effect of WBC contamination in serum samples on the serum *M/N* ratio, we measured the serum *M/N* ratio using DNA extracted from a series of WBC-contaminated serum samples. The samples were prepared by adding 0, 1 × 10, 1 × 10^2, 1 × 10^3, 1 × 10^4, and 1 × 10^5 of WBCs from a healthy donor to 200 μL of serum from a *MYCN*-amplified patient.

Statistical Methods

The difference in the serum *M/N* ratio between the MNA and non-MNA groups was assessed using the Mann-Whitney *U* test. $P < .05$ was judged as significant.

Serum M/N Ratio As a Predictor of MYCN Status of Tumor

Serum *M/N* ratios could be determined in approximately 4 hours by real-time quantitative PCR. Figure 1 shows the distribution of the serum *M/N* ratio in the MNA and non-MNA groups at the time of diagnosis. The serum *M/N* ratio in the MNA group (n = 17; median, 199.32; range, 17.1 to 901.6; 99% CI, 107.0 to 528.7) was significantly ($P < .001$) higher than the ratio in the non-MNA group (n = 70; median, 0.87; range, 0.25 to 4.6; 99% CI, 0.82 to 1.26). In fact, there was no overlap between the two groups in the limited number of patients examined in this study. As a cutoff for the serum *M/N* ratio to distinguish between MNA and non-MNA patients, we empirically chose a value of 10, which was in the middle of the two ranges. With this value, the sensitivity and specificity of the serum *M/N* ratio as a diagnostic test to distinguish patients with MNA from those without MNA were both 100% for our limited number of patients. That is, the serum *M/N* ratio was in complete agreement with the Southern blotting results. The positive and negative predictive values were 100%. The serum *M/N* ratios were also consistent with results obtained by FISH for 45 of the patients (FISH analyses were performed in 12 of the 17 MNA patients and in 33 of the 70 nonamplified patients). Three of the patients who had one to four extra copies of the *MYCN* gene relative to chromosome 2 centromere number, as determined by FISH, also had slightly elevated serum *M/N* ratios (2.5, 3.3, and 4.6).

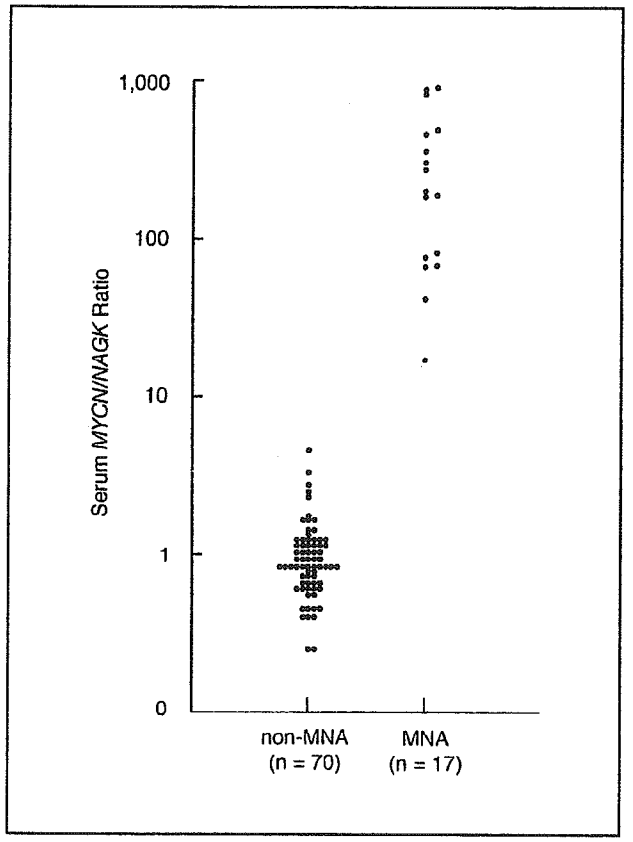

Fig 1. A scatter plot of serum *MYCN/NAGK* ratio in patients with *MYCN*-amplified (MNA) and nonamplified (non-MNA) neuroblastoma. The serum *MYCN/NAGK* ratio was significantly ($P < .001$) higher in the MNA group (median, 199.32; range, 17.1 to 901.6; 99% CI, 107.0 to 528.7) than in the non-MNA group (median, 0.87; range, 0.25 to 4.6; 99% CI, 0.82 to 1.26; Mann-Whitney *U* test).

Change in Serum M/N Ratio Levels During Follow-Up

To evaluate whether an increase in the serum *M/N* ratio can be used as an indicator of relapse, we measured serum *M/N* ratios at several points in the clinical courses of six patients with MNA (Fig 2). In three patients who were in complete remission (patients 1, 2, and 3), the serum *M/N* ratios decreased to the normal range and were consistently low. In contrast, in one patient who failed to achieve remission (patient 4), the serum *M/N* ratio did not decrease to the normal range and remained at a high level until his death. In the other patients who experienced recurrence after remission (patients 5 and 6), the serum *M/N* ratio first decreased to the normal range and then increased beyond the cutoff value by the time of diagnosis.

Effect of WBC Contamination on Serum M/N Ratio

We found that a high serum *M/N* ratio could be masked by the presence of WBC. The *M/N* ratio of serum from an *MYCN*-amplified patient decreased with increasing WBC contamination (Fig 3). When 200 μL of serum was contaminated with 1×10^5 of WBC, corresponding to approximately one fortieth of the WBC concentration in normal whole blood, the serum *M/N* ratio decreased below the cutoff level.

Serum markers, such as ferritin,[19] lactic dehydrogenase,[20] and neuron-specific enolase,[21] have been proposed as prognostic markers of NB, although they have shown little prognostic value. Recently, elevated levels of plasma midkine have been reported to correlate with a poor prognosis. However, the significance of this finding is controversial because plasma midkine levels are highest in stage 4S patients.[22] Therefore, a noninvasive assay of tumor-related

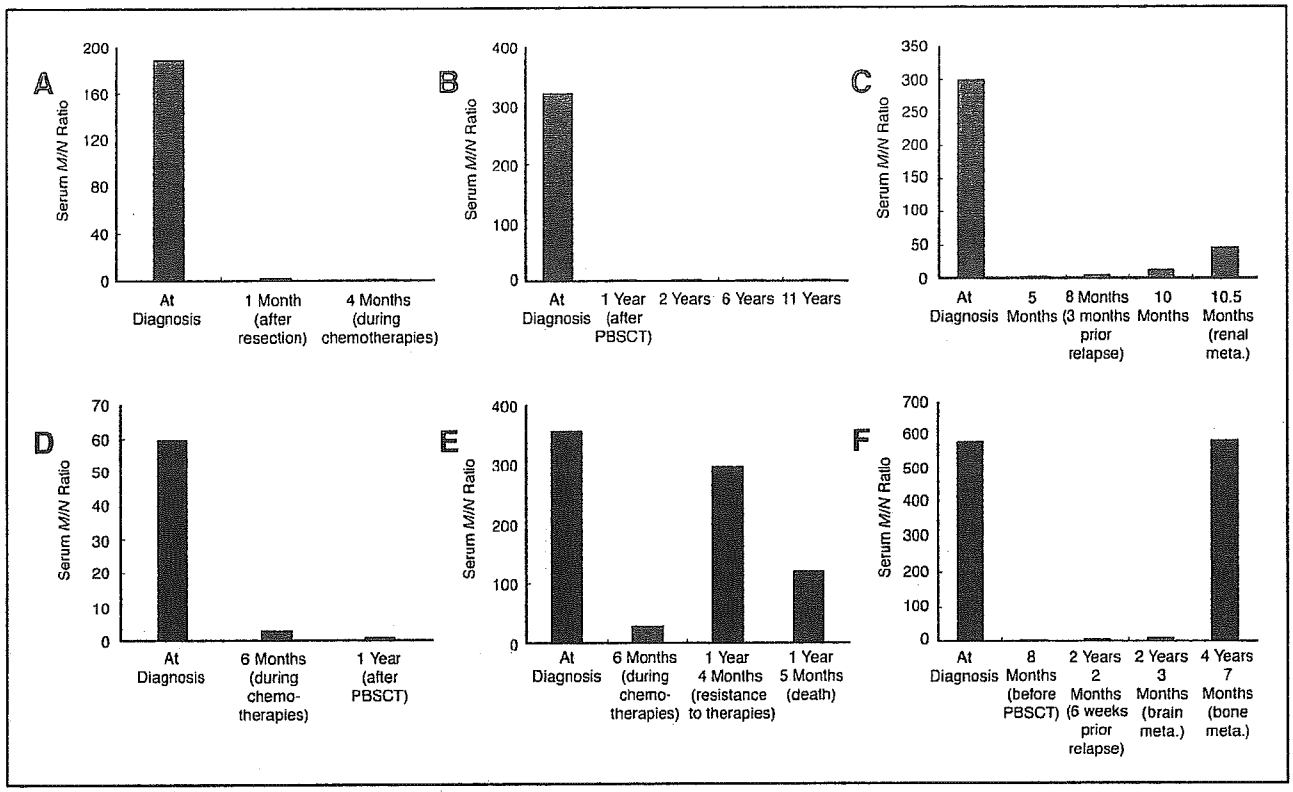

Fig 2. Changes in serum *MYCN/NAGK* (*M/N*) ratio levels of six patients with *MYCN* amplification during follow-up. PBSCT, peripheral-blood stem-cell transfusion; meta., metastasis. (A) Patient 1; (B) patient 3; (C) patient 5; (D) patient 2; (E) patient 4; (F) patient 6.

genetic aberrations using serum DNA is desirable for the assessment of prognosis and therapy stratification at the time of diagnosis. Among the tumor-related genetic aberrations detected in NB, MNA was of greatest interest to us because of its significant prognostic value.

By using DNA-based real-time quantitative PCR with a single-copy reference gene, we have demonstrated that the *M/N* ratio in serum DNA is a valuable diagnostic tool to discriminate MNA patients from non-MNA patients. The serum *M/N* ratio in the MNA group was significantly higher than the ratio in the non-MNA group, without an overlap. The highest sensitivity (100%), highest specificity (100%), highest positive predictive value (100%), and highest negative predictive value (100%) were obtained with a serum *M/N* ratio cutoff value of 10.0. Furthermore, we found an elevated level of the serum *M/N* ratio in a stage 1 patient and a stage 2B patient with MNA (188.7 and 901.6, respectively), even though the tumor was localized in these patients. This suggests that tumors could release a significant amount of genomic DNA into the systemic circulation even at an early stage. Furthermore, Sozzi et al[23] reported that the concentration of plasma DNA in 84 lung cancer patients was higher than the concentration in 43 controls, regardless of the tumor stage, and suggested that circulating DNA in peripheral blood was an early event in lung carcinogenesis.

Another clinical benefit of the serum *M/N* assay is that it could be used as a marker to monitor therapeutic efficacy and recurrence after therapies. The serum *M/N* ratio decreased to the normal range in the patients in remission but remained at a high level in the patient who failed to achieve remission. Furthermore, in two patients with recurrence after remission, the serum *M/N* ratio initially decreased to the normal range but then increased beyond the cutoff value by the time of diagnosis. The serum *M/N* ratio did not increase to the initial level as long as the metastasis was localized in the brain, but it did increase to the initial level when the patient later developed a bone metastasis (patient 6). This is noteworthy because it suggests that a brain metastasis releases genomic DNA into the systemic circulation less easily than extracranial tumors. If this is confirmed by examination of additional patients, then it is possible that tumors localized in brain could be overlooked with diagnostic assays based on serum DNA.

A possible pitfall of our serum *M/N* assay is that a high serum *M/N* ratio could be reduced by WBC contamination (Fig 3). This could be a result of dilution of tumor DNA with the WBC DNA, which would be expected to have an *M/N* ratio of 1. Therefore, the importance of removing WBCs from serum should be addressed in diagnostic assays

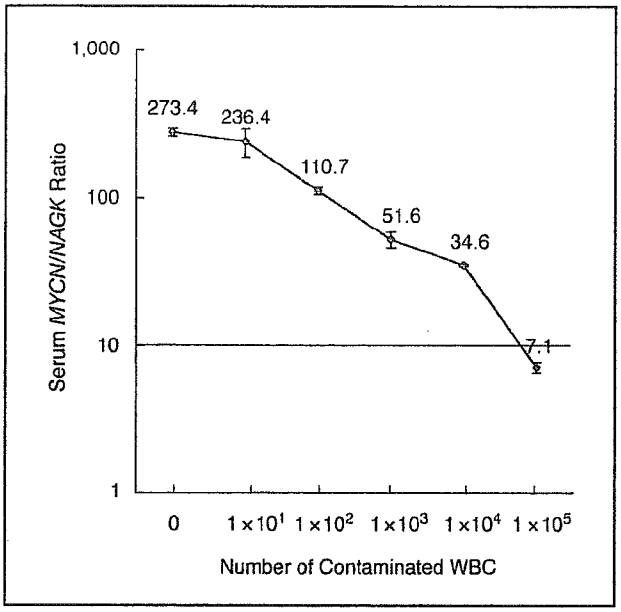

Fig 3. Influence of WBC contamination in serum samples on the serum *MYCN/NAGK* ratio. Data are presented as the mean ± standard deviation of duplicate measurements. The transverse line represents a *MYCN/NAGK* ratio cutoff value of 10.0.

that use serum DNA. For the same reason, a predominance of any nontumor DNA in serum may lower an elevated *M/N* ratio of an *MYCN*-amplified patient. However, this assay can be accurate on the premise that, in cancer patients, serum DNA predominantly consists of tumor-released DNA.[7] In addition, the use of serum DNA as a diagnostic tool in lung cancer patients has resulted in a diversity of findings, suggesting that these differences likely reflect variations in the manner in which the blood specimens were collected and handled and variations in the methods by which the assay were conducted.[24] Therefore, it is necessary to standardize the serum collection procedure to ensure that different laboratories obtain the same result with a given blood sample. An additional high-speed centrifugation step (16,000 × *g* for 5 minutes) was found to eliminate cellular contamination even after thawing of stored samples.[25] By using the appropriate centrifugation methods, we believe that WBC-free serum can be reliably achieved.

Although a large set of patients needs to be studied to verify the accuracy of this assay and to set an appropriate cutoff, our results are promising and need to be further tested. The advantages of this method are that it takes only 4 hours and much less effort than FISH and Southern blotting, which should make this assay an alternative to these other methods for determining *MYCN* status. A third advantage is that the serum *M/N* ratio seems to be a promising indicator of therapeutic efficacy and relapse in the follow-up of patients with MNA, although more patients need to be examined to confirm its reliability.

Acknowledgment

We thank two anonymous reviewers for helpful comments.

Authors' Disclosures of Potential Conflicts of Interest

The authors indicated no potential conflicts of interest.

1. Brodeur GM, Seeger RC, Schwab M, et al: Amplification of N-myc in untreated human neuroblastomas correlates with advanced disease stage. Science 224:1121-1124, 1984
2. Seeger RC, Brodeur GM, Sather H, et al: Association of multiple copies of the N-myc oncogene with rapid progression of neuroblastomas. N Engl J Med 313:1111-1116, 1985
3. Brodeur GM, Maris JM, Yamashiro DJ, et al: Biology and genetics of human neuroblastomas. J Pediatr Hematol Oncol 19:93-101, 1997
4. Brodeur GM, Pritchard J, Berthold F, et al: Revisions of the international criteria for neuroblastoma diagnosis, staging and response to treatment. J Clin Oncol 11:1466-1477, 1993
5. Castleberry RP, Prichard J, Ambros P, et al: The International Neuroblastoma Risk Groups (INRG): A preliminary report. Eur J Cancer 33: 2113-2116, 1997
6. Shimada H, Ambros IM, Dehner LP, et al: The International Neuroblastoma Pathology Classification System (the Shimada system). Cancer 86:364-372, 1999
7. Shapiro B, Chakrabarty M, Cohn EM, et al: Determination of circulating DNA levels in patients with benign or malignant gastrointestinal disease. Cancer 51:2116-2120, 1983
8. Sozzi G, Conte D, Leon M, et al: Quantification of free circulating DNA as a diagnostic marker in lung cancer. J Clin Oncol 21:3902-3908, 2003
9. Sozzi G, Musso K, Ratcliffe C, et al: Detection of microsatellite alterations in plasma DNA of non-small cell lung cancer patients: A prospect for early diagnosis. Clin Cancer Res 5:2689-2692, 1999
10. Chen X, Bonnefoi H, Diebold-Berger S, et al: Detecting tumor-related alterations in plasma or serum DNA of patients diagnosed with breast cancer. Clin Cancer Res 5:2297-2303, 1999
11. Silva JM, Dominguez G, Garcia JM, et al: Presence of tumor DNA in plasma of breast cancer patients: Clinicopathological correlations. Cancer Res 59:3251-3256, 1999
12. Combaret V, Audoynaud C, Iacono I, et al: Circulating *MYCN* DNA as a tumor-specific marker in neuroblastoma patients. Cancer Res 62:3646-3648, 2002
13. Akiyama K, Kanda N, Yamada M, et al: Megabase-scale analysis of the origin of N-myc amplicons in human neuroblastoma. Nucleic Acids Res 22:187-193, 1994
14. Gotoh T, Sugihara H, Matsumura T, et al: Human neuroblastoma demonstrating clonal evolution in vivo. Genes Chromosomes Cancer 22:42-49, 1998
15. Spitz R, Hero B, Skowron M, et al: *MYCN*-status in neuroblastoma: Characteristics of tumours showing amplification, gain, and non-amplification. Eur J Cancer 40:2753-2759, 2004
16. Gelmini S, Orlando C, Sestini R, et al: Quantitative polymerase chain reaction-based homogeneous assay with fluorogenic probes to measure c-erbB-2 oncogene amplification. Clin Chem 43:752-758, 1997
17. Claudia CR, Maria LB, Gian PT, et al: Real-time quantitative PCR for the measurement of *MYCN* amplification in human neuroblastoma with the TaqMan detection system. Clin Chem 45:1918-1924, 1999
18. Chiang PW, Beer DG, Wei WL, et al: Detection of erbB-2 amplifications in tumors and sera from esophageal carcinoma patients. Clin Cancer Res 5:1381-1386, 1999
19. Hann HWL, Evans AE, Siegel SE, et al: Prognostic importance of serum ferritin in patients with stage III and IV neuroblastoma: The

Children's Cancer Study Group experience. Cancer Res 45:2843-2848, 1985

20. Quinn JJ, Altman AJ, Frantz CN, et al: Serum lactic dehydrogenase, an indicator of tumor activity in neuroblastoma. J Pediatr 97:89-91, 1980

21. Massaron S, Seregni E, Luksch R, et al: Neuron-specific enolase evaluation in patients neuroblastoma. Tumour Biol 19:261-268, 1998

22. Ikematsu S, Nakagawara A, Nakamura Y, et al: Correlation of elevated level of blood midkine with poor prognostic factors of human neuroblastomas. Br J Cancer 88:1522-1526, 2003

23. Sozzi G, Conte D, Mariani L, et al: Analysis of circulating tumor DNA in plasma at diagnosis and during follow-up of lung cancer patients. Cancer Res 61:4675-4678, 2001

24. Bunn PA: Early detection of lung cancer using serum RNA or DNA markers: Ready for "prime time" or for validation? J Clin Oncol 21:3891-3893, 2003

25. Swinkels DW, Wiegerinck E, Steegers EAP, et al: Effect of blood-processing protocols on cell-free DNA quantification in plasma. Clin Chem 49:525-526, 2003

Methylation-Associated Silencing of the *Nuclear Receptor 1I2* Gene in Advanced-Type Neuroblastomas, Identified by Bacterial Artificial Chromosome Array-Based Methylated CpG Island Amplification

Akiko Misawa,[1,4] Jun Inoue,[1,4] Yuriko Sugino,[1,4,5] Hajime Hosoi,[5] Tohru Sugimoto,[5] Fumie Hosoda,[3] Misao Ohki,[3] Issei Imoto,[1,4] and Johji Inazawa[1,2,4]

[1]Department of Molecular Cytogenetics, Medical Research Institute and Graduate School of Biomedical Science and [2]Center of Excellence Program for Frontier Research on Molecular Destruction and Reconstitution of Tooth and Bone, Tokyo Medical and Dental University; [3]Cancer Genomics Project, National Cancer Center Research Institute, Tokyo, Japan; [4]Core Research for Evolutionary Science and Technology of the Japan Science and Technology Corporation, Saitama, Japan; and [5]Department of Pediatrics, Kyoto Prefectural University of Medicine, Kyoto, Japan

Abstract

To identify genes whose expression patterns are altered by methylation of DNA, we established a method for scanning human genomes for methylated DNA sequences, namely bacterial artificial chromosome array-based methylated CpG island amplification (BAMCA). In the course of a program using BAMCA to screen neuroblastoma cell lines for aberrant DNA methylation compared with stage I primary neuroblastoma tumors, we identified CpG methylation-dependent silencing of the *nuclear receptor 1I2* (*NR1I2*) gene. *NR1I2* was methylated in a subset of neuroblastoma cell lines and also in advanced-stage primary tumors with amplification of *MYCN*. Its methylation status was inversely associated with gene expression. Treatment with the demethylating agent 5-aza-2′-deoxycytidine restored *NR1I2* transcription in neuroblastoma cell lines lacking endogenous expression of this gene. A CpG island located around exon 3 of *NR1I2* showed promoter activity, and its methylation status was clearly and inversely correlated with *NR1I2* expression status. The gene product, NR1I2, has a known function in regulating response to xenobiotic agents but it also suppressed growth of neuroblastoma cells in our experiments. We identified some possible transcriptional targets of NR1I2 by expression array analysis. The high prevalence of *NR1I2* silencing by methylation in aggressive neuroblastomas, together with the growth-suppressive activity of NR1I2, suggests that this molecule could serve as a diagnostic marker to predict prognosis for neuroblastomas. (Cancer Res 2005; 65(22): 10233-42)

Introduction

Neuroblastoma, the most common extracranial solid tumor of childhood, has distinct biological characteristics in different prognostic subgroups. Children (>12 months at diagnosis) with stage IV or *MYCN*-amplified stage III tumors are at high risk of mortality (>60%), children with non-*MYCN*-amplified local-regional tumors (i.e., stages I, II, and III) and infants (<12 months at diagnosis) with stage IVS disease are generally at low risk of mortality (<10%), and infants with stage IV disease and children with stage III disease without *MYCN* amplification are at intermediate risk (1, 2), although the biological basis for that clinical diversity remains unclear. In addition to genetic changes including the *MYCN* amplification, epigenetic alterations often play important roles in the pathogenesis of human cancers, including neuroblastoma (3). For example, hypermethylation of promoter sequences of *CASP8, RASSF1A, CD44, TSP-1*, and *HSP47* genes has been observed in neuroblastoma tumors (4–8), and silencing of *CASP8* through methylation of its promoter tends to be associated with *MYCN* amplification (4). A reported positive correlation between promoter hypermethylation of *CASP8* and *RASSF1A* (5) suggests that hypermethylation of multiple genes may influence the phenotype of neuroblastoma.

Because hypermethylation in CpG-rich promoter or exonic regions seems to be a critical contributor to inactivation of tumor suppressor genes in many human cancers through transcriptional silencing (9), identification of hypermethylated CpG-rich sequence in cancer cell genomes could accelerate identification of unknown tumor suppressors. Although several techniques, including a method known as methylated CpG island amplification (MCA), have been developed (10, 11), we still have limited number of effective and practical high-throughput methods for genome-wide screening of aberrantly methylated CpG-rich sequences. To accomplish high-throughput screening for methylated sites in the entire genome, we developed a bacterial artificial chromosome (BAC) array-based MCA (BAMCA), incorporating our custom-made, BAC-based genomic DNA array combined with MCA (12).

In an effort to identify genes that are silenced by methylation mechanisms and associated with progression of neuroblastoma, we applied BAMCA to human neuroblastoma in the study reported here. Because the pattern of genomic changes observed in most neuroblastoma-derived cell lines is similar to that of advanced primary neuroblastomas (13), we used DNAs from neuroblastoma cell lines and from stage I primary tumors as test and reference samples, respectively. Using this approach, we successfully identified one gene, *nuclear receptor 1I2* (*NR1I2*), also known as *PXR*, whose expression was decreased in a subset of

Note: A. Misawa and J. Inoue contributed equally to this work.

Supplementary data for this article are available at Cancer Research Online (http://cancerres.aacrjournals.org/).

Requests for reprints: Johji Inazawa, Department of Molecular Cytogenetics, Medical Research Institute, Tokyo Medical and Dental University, 1-5-45 Yushima, Bunkyo-ku, 113-8510 Tokyo, Japan. Phone: 81-3-5803-5820; Fax: 81-3-5803-0244; E-mail: johinaz.cgen@mri.tmd.ac.jp.

doi:10.1158/0008-5472.CAN-05-1073

human cell lines and tumors of neuroblastoma through hypermethylation of a CpG island showing promoter activity. *NR1I2* was methylated and silenced mainly in late-stage neuroblastoma tumors with *MYCN* amplification and in older children. Exogenous restoration of NR1I2 expression suppressed growth of neuroblastoma cells lacking endogenous expression of the gene.

Materials and Methods

Cell culture, drug treatment, and primary tissue samples. All 19 human neuroblastoma cell lines we used (SK-N-KS, SK-N-AS, SK-N-SH, SK-N-DZ, SH-SY5Y, MP-N-TS, MP-N-MS, KP-N-RT, KP-N-SIFA, KP-N-SILA, KP-N-TK, KP-N-YS, SMS-KCN, SMS-KAN, SJ-N-CG, NB-1, CHP134, IMR32, and GOTO) had been established from surgically resected tumors and maintained as described previously (13). These cultures

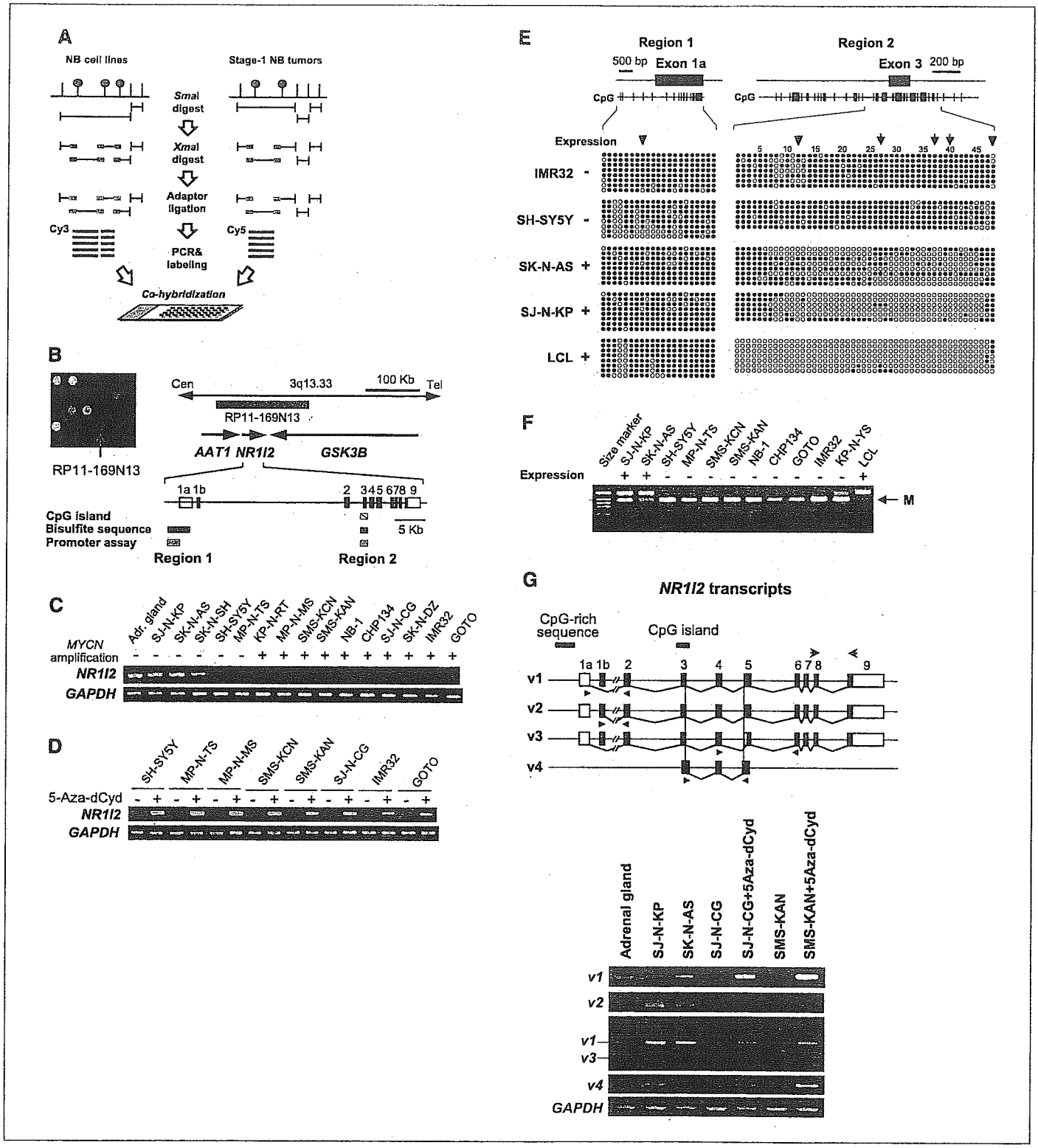

were treated with or without 1 μmol/L 5-aza 2′-deoxycytidine (5-aza-dCyd) for 5 days.

Primary tumor samples were obtained at surgery from 51 neuroblastoma patients who underwent tumor resection at University Hospital, Kyoto Prefectural University of Medicine from 1986 to 2003, with written consent from the parents of each patient in the formal style and after approval by the local ethics committees. Staging was evaluated according to the criteria of the International Neuroblastoma Staging System (14). Of the 51 cases, 12 were classified as stage I, 11 as stage II, eight as stage III, 13 as stage IV, and four as stage IVS. Thirty-seven of the patients were infants <1 year of age at diagnosis. *MYCN* amplification was detected in 8 of 51 cases (15%). In 39 cases (76%), neuroblastoma had been detected by a mass screening program. Patients were treated according to previously described protocols (15, 16). Tumor samples were frozen immediately and stored at −80°C until required.

Bacterial artificial chromosome array-based methylated CpG island amplification. The preparation of DNA probes for screening of methylated regions was carried out by the MCA method described by Toyota et al. (11). Five-microgram aliquots of test DNA were first digested with 100 units of a methylation-sensitive restriction enzyme *Sma*I and subsequently with 20 units of methylation-insensitive *Xma*I. Adaptors were ligated to *Xma*I-digested sticky ends and PCRs were done with an adaptor primer and Cy3-dCTP for labeling. Control DNA was treated in the same manner except that labeling was with Cy5-dCTP (Fig. 1*A*).

Labeled test and control PCR products were cohybridized to our in-house array (MCG Whole Genome Array-4500; ref. 12). Hybridizations were carried out as described elsewhere (17). Arrays were scanned with a GenePix 4000B (Axon Instruments, Foster City, CA) and analyzed using GenePix Pro 4.1 software (Axon Instruments).

Reverse transcription-PCR and real-time quantitative reverse transcription-PCR. Single-stranded cDNAs were generated from total RNAs (17) and amplified with specific primers for each gene. Primer sequences are available on request. Real-time quantitative PCR was done using LightCycler (Roche Diagnostics, Tokyo, Japan) with SYBR green as described previously (18). The *glyceraldehyde-3-phosphate dehydrogenase* (*GAPDH*) gene served as an endogenous control. Each sample was normalized on the basis of its *GAPDH* content. PCR amplification was done in duplicate for each sample.

Methylation analysis. To investigate methylation of DNA, the method of combined bisulfite restriction analysis (COBRA) was done as described earlier (11). Genomic DNAs were treated with sodium bisulfite and subjected to PCR using primer sets designed to amplify the regions of interest. PCR products were digested with *Hha*I, which recognizes sequences unique to the methylated alleles but cannot recognize unmethylated alleles, and electrophoresed. For bisulfite sequencing, PCR products were subcloned and sequenced.

Reporter assay. A 1,060 bp fragment upstream of exon 1 of *NR1I2* (region 1; Fig. 1*A*) and a 480 bp fragment of a CpG island that includes exon 3 (region 2; Fig. 1*A*) were ligated into the pGL3-Basic vector (Promega, Madison, WI) in front of and/or downstream of the luciferase gene. An equal amount of each construct was introduced into cells with an internal control vector (pRL-hTK, Promega), using FuGENE 6 (Roche Diagnostics). A pGL3-Basic vector without insert served as a negative control. Firefly luciferase and *Renilla* luciferase activities were each measured 36 hours after transfection using the Dual-Luciferase Reporter Assay System (Promega); relative luciferase activities were calculated and normalized versus *Renilla* luciferase activity.

Transfection, Western blotting, and colony formation assays. A full-length *NR1I2* cDNA was cloned into the pCMV-Tag3 eukaryotic expression vector (Stratagene, La Jolla, CA) with or without etoposide (VP-16) in-frame along with the Myc epitope. A plasmid expressing a Myc-tagged NR1I2 with or without VP-16 (pCMV-Tag3-VP-*NR1I2* or pCMV-Tag3-*NR1I2*), or the empty vector (pCMV-Tag3-mock), were transfected into cells using FuGENE6 (Roche Diagnostics). Expression of NR1I2 protein in transfected cells was confirmed by Western blotting using anti-Myc-Tag antibody (9B11; Cell Signaling Technology, Beverly, MA). For colony formation assays, transfected cells were selected with 500 μg/mL G418; 3 weeks after transfection, the neomycin-resistant colonies were stained with crystal violet and counted (17).

Cell growth assay. Stable NR1I2 transfectants and controls were obtained by transfecting pCMV-Tag3-VP-*NR1I2* or pCMV-Tag3-mock, respectively, into cells lacking *NR1I2* expression. For measurements of cell growth, 2×10^3 cells were seeded in 96-well plates. The numbers of viable cells were assessed by a colorimetric water-soluble tetrazolium salt assay (cell counting kit-8; Dojindo Laboratories, Kumamoto, Japan).

Oligonucleotide array analysis. mRNA expression profiling was done using the AceGene Human oligo chip 30K (DNA Chip Research, Inc., Kanagawa, Japan), containing 30,000 genes, as described elsewhere (18). The test and reference cDNA probes labeled with aminoallyl-dUTP (Ambion, Inc., Austin, TX) were synthesized using oligo(dT)12-18 primer and coupled with Cy3- or Cy5-monoreactive dye (Amersham Biosciences, Tokyo, Japan), respectively. The hybridized chips were scanned using GenePix 4000B (Axon Instruments) and analyzed using GenePix Pro 4.1 software (Axon Instruments). Signal intensities between the two fluorescent images were normalized by the averaged values for blank spots; this procedure effectively defined the signal intensity-weighted spot for the internal controls of housekeeping genes on each array to have a Cy3/Cy5 ratio of 1.0.

Results

Methylation analysis of neuroblastoma cell lines by bacterial artificial chromosome array-based methylated CpG island amplification. To assess DNA methylation in the more advanced type of neuroblastoma tumors, we did BAMCA

Figure 1. Methylation status and expression levels of *NR1I2* in neuroblastoma (*NB*) cell lines. *A*, BAMCA procedure. The DNAs from neuroblastoma cell lines (test) or stage I neuroblastoma tumors (control) were first digested with *Sma*I in the blunt end and subsequently with *Xma*I in the sticky end (*blue boxes*). Adaptors were ligated to *Xma*I-digested sticky ends (*pink boxes*) and PCR was done with an adaptor primer and Cy3-dCTP (test) or Cy5-dCTP (control) for labeling. Labeled PCR products were cohybridized to BAC array. *B*, *left*, representative image of BAMCA analysis applied to the IMR32 cell line. *Green*, BAC containing highly methylated fragments in IMR32 compared with stage I tumors; *red*, BAC containing highly methylated fragments in stage I tumors compared with IMR32; *yellow*, unchanged methylation status; *black*, no detectable methylated fragments. The RP11-169N13 BAC (*arrow*) harboring *NR1I2* was detected as spot with a high Cy3 (test)/Cy5 (control) ratio. *Right*, genomic structure of the *NR1I2* gene consisting of nine exons. A 239 bp CpG island exists around exon 3 (Genbank accession nos. NM_003889 for cDNA sequence and NT_005612 for genomic sequence). *Horizontal bars*, regions examined in a promoter assay and bisulfite sequencing analysis (regions 1 and 2). *C*, representative results of RT-PCR analysis of *NR1I2* mRNA expression in normal adrenal gland and neuroblastoma cell lines with (+) or without (−) amplification of *MYCN*. *GAPDH* was used as an internal control. *D*, representative results of RT-PCR analysis to reveal *NR1I2* expression in neuroblastoma cell lines with (+) and without (−) treatment with 5-aza-dCyd. *GAPDH* was used as an internal control. *E*, *top*, map of the 5′ region (exon 1 and upstream sequence, region 1) and the CpG island around exon 3 (region 2) in *NR1I2*. *Vertical tick marks*, CpG sites. *Bottom*, results of bisulfite sequencing analysis done in *NR1I2*-nonexpressing cell lines (IMR32 and SH-SY5Y) and *NR1I2*-expressing cell lines (SK-N-AS, SJ-N-KP, and LCL). ○, unmethylated CpG sites; ●, methylated CpG sites, respectively; each row represents a single clone. *Arrows*, *Hha*I restriction site. *Arrowheads*, *Sma*I restriction site. *F*, representative results of COBRA of region 2 in neuroblastoma cell lines with (+) or without (−) *NR1I2* expression. A 492 bp PCR product, including exon 3, was restricted by *Hha*I. *M*, methylated alleles. *G*, *top*, map of four variants (*v1-v4*) and location of each primer set used for RT-PCR analysis. *Black boxes*, coding exons; *gray box*, deleted region in variant 3. *Arrows*, primers used for RT-PCR shown in (*B* and *C*), and in Fig. 2*B* and *C*; *arrowheads*, primer sets specific for each variant. Nucleotide sequences for primers used are available on request. *Bottom*, representative results of RT-PCR analysis. A primer set for variant 3 amplified two products with 441 and 330 bp sizes from variants 1 and 3, respectively.

Table 1. List of positive BACs in BAMCA analysis and summary of screening of candidate methylated genes

	BAC (RP11)	Locus	Gene		CpG island*
			Symbol	Name	
1	73D7	*1q32.1*	*LHX9*	*LIM homeobox 9*	+
2	451A14	*2p24*	No gene		
3	169N13	*3q13.3*	*NR1I2*	*Nuclear receptor subfamily 1, 2group I, member 2*	+
			GSK3B	*Glycogen synthase kinase 3β*	−
			AAT1	*AAT1-α*	−
4	205N12	*4p15.1*	*PCDH7*	*Protocadherin 7*	+
5	17P19	*4q21.2*	*MRPL1*	*Mitochondrial ribosomal protein L1*	−
6	611D20	*9q34*	*NOTCH1*	*Notch homologue 1, translocation-associated (Drosophila)*	+
7	248C1	*10q23.33*	*MPHOSPH1*	*M-phase phosphoprotein 1*	+
8	37L21	*10q24*	*SEMA4G*	*Sema domain, immunoglobulin domain, transmembrane domain and short cytoplasmic domain (semaphorin) 4G*	+
			MRPL43	*Mitochondrial ribosomal protein L43*	+
9	23E5	*11p15.1*	*DELGEF*	*Deafness locus associated putative guanine nucleotide exchange factor*	+
10	56E13	*11p11.2*	*PTPRJ*	*Protein tyrosine phosphatase, receptor type, J*	+
11	79L5	*18q21.2*	*ONECUT2*	*One cut domain, family member 2*	+
12	7F10	*20p11.22*	*PAX1*	*Paired box gene 1*	+
13	124D1	*20q13*	*PREX1*	*Phosphatidylinositol 3,4,5-trisphosphate-dependent RAC exchanger 1*	+
14	93B14	*20q13.33*	*FLJ32154*	*unknown*	+
			SLCO4A1	*Solute carrier organic anion transporter family, member 4A1*	+
			NTSR1	*Neurotensin receptor 1 (high affinity)*	+
15	58O1	*10q22.1*	*SLC29A3*	*Solute carrier family 29 (nucleoside transporters), member 3*	+
			UNC5B	*Unc-5 homologue B (Caenorhabditis elegans)*	+
16	88B12	*10q26.2*	*MGC32871*	*Hypothetical protein*	−
			PTPRE	*Protein tyrosine phosphatase, receptor type, E*	+
17	262M8	*14q21.3*	*PTGDR*	*Prostaglandin D2 receptor*	+
			PTGER2	*Prostaglandin E receptor 2 (subtype EP2), 53 kDa*	+
18	79J21	*15q24*	*ETFA*	*Electron-transfer-flavoprotein, αpolypeptide (glutaric aciduria II)*	−
			ISL2	*ISL2 transcription factor, LIM/homeodomain, (islet-2)*	+

*CpG islands were searched using NCBI human genome database (http://www.ncbi.nlm.nih.gov/).
†Each Cy3-labeled neuroblastoma cell line sample/Cy5-labeled mixed stage I neuroblastoma tumor samples (see Fig. 1*A*).
‡Methylation status in primary tumors was determined by using bisulfite-PCR analysis (see Fig. 2*A*). −, ≤5%; ±, >5% and ≤50%; +, >50%.
§GOTO cells were treated with 1 μmol/L of 5-aza-dCyd for 5 days (see Fig. 1*C*).

(Fig. 1*A*) with our MCG Whole Genome Array-4500 (12) using DNA from each of two neuroblastoma cell lines (IMR32 and GOTO) and mixed DNA from five stage I primary neuroblastoma tumors as test and control DNAs, respectively. As shown in Table 1, 18 BACs, which contain 24 known genes and two uncharacterized transcripts, showed high Cy3 (test)/Cy5 (control) ratios (>1.5) by BAMCA in both cell lines, and were selected as sequences whose CpG sites were frequently methylated in advanced types of neuroblastoma tumors. The same result was obtained in the repeated experiments using the same samples (data not shown), suggesting that BAMCA is a reproducible method. We then selected possible candidates by sequentially analyzing the following: (*a*) the expression status of each gene in stage I primary neuroblastoma tumors and in IMR32 and GOTO cells; (*b*) restoration of gene expression after treatment with 5-aza-dCyd; and (*c*) methylation status of CpG islands around each candidate gene in stage I and stage IVa primary neuroblastoma tumors (data not shown). As shown in Table 1, *NR1I2* located within RP11-169N13 (Fig. 1*B*) emerged as a gene that was (*a*) expressed in stage I tumors but not in the two neuroblastoma cell lines, (*b*) restored after treatment with 5-aza-dCyd, and (*c*) frequently methylated in stage IVa tumors but infrequently in stage I tumors. Those results prompted us to perform detailed analysis of the *NR1I2* gene as a putative tumor suppressor whose silencing by a DNA methylation mechanism might be associated with progression of neuroblastoma.

Analysis of *NR1I2* expression in neuroblastoma cell lines. When we examined *NR1I2* expression in our panel of 19 neuroblastoma cell lines by reverse transcription-PCR (RT-PCR; Fig. 1*C*), no *NR1I2* mRNA was detected in 14 of the lines (73%): in 11 of 12 *MYCN* amplified lines (91%) or in 3 of 7 *MYCN* nonamplified lines (43%). One line, MP-N-TS, lacking expression of *NR1I2* and without *MYCN* amplification, does show c-*MYC* amplification (13). Normal adrenal gland, which is considered the tissue of origin for neuroblastoma tumors, expressed *NR1I2* mRNA.

To investigate whether demethylation could restore *NR1I2* mRNA in neuroblastoma cells lacking endogenous expression, we treated cells with 1 μmol/L of 5-aza-dCyd, a methyltransferase inhibitor, for 5 days. Expression of *NR1I2* mRNA was remarkably increased after the treatment (Fig. 1*D*).

Table 1. List of positive BACs in BAMCA analysis and summary of screening of candidate methylated genes (Cont'd)

BAMCA ratio[†]		mRNA expression				Methylation[‡]	
GOTO	IMR32	Stage I	IMR32	GOTO	GOTO (+5-aza-dCyd)[§]	Stage I	Stage IVa
3.46	4.57	−	+	+			
1.91	10.78						
1.68	2.10	+	−	−	+	−	+
		+	+	+			
		+	+	+			
3.01	5.19	+	+	+			
2.10	2.05	+	+	+			
1.72	2.33	+	+	+			
3.07	5.54	+	+	+			
2.54	2.32	+	+				
		+	+	+			
3.52	2.17	+	−	+			
3.31	2.48	+	−	−	−		
3.89	5.45	+	+	+			
3.72	12.90	+	−	+			
2.06	1.45	+	+	+			
2.51	3.51	−	−	−			
		+	+	+			
		+	+	−			
1.81	1.85	+	+	+			
		+	+	+			
1.75	16.90	+	−	−	−		
		+	−	−	±	−	±
2.93	3.24	+	−	−	+	−	±
		+	−	−	+	−	±
1.54	3.39	+	+	+			
		−	+	+			

Methylation of *NR1I2* CpG island in neuroblastoma cell lines. We next examined the methylation status of the slightly CpG-rich 5′ region (region 1) and the CpG island including exon 3 (region 2) of the *NR1I2* gene, which had been detected by the National Center for Biotechnology Information (NCBI) human genome database[6] as shown in Fig. 1*E*. Bisulfite sequencing analysis of region 2 revealed aberrant DNA hypermethylation in IMR32 and SH-SY5Y cell lines lacking expression of *NR1I2*, but hypomethylation in two lines expressing the gene (SK-N-AS and SK-N-KP) and in a normal lymphoblast cell line (LCL). On the other hand, no significant difference in methylation pattern within region 1 was observed among those four neuroblastoma cell lines and LCL, regardless of expression status. We did COBRA to confirm the relationship between expression and methylation status within region 2 in a larger set of neuroblastoma cell lines. Predominant methylated alleles were detected in all lines lacking *NR1I2* expression (Fig. 1*F* and data not shown).

Because several splicing variants of *NR1I2*, including the variant starting transcription from exon 3 (variant 4, v4), have been reported in various human tissues (19),[7] we did RT-PCR using specific primers for each variant to examine which transcripts might be silenced through a DNA methylation within region 2 in neuroblastoma cell lines (Fig. 1*G*). Variant 1, the most major variant in various human tissues, and variant 2 were expressed in unmethylated neuroblastoma cell lines, but not in methylated lines, whereas variant 4 without open reading frame was not expressed in one of the unmethylated cell lines (SK-N-AS). The expression of variant 1 and variant 4 was restored after the treatment with 5-aza-dCyd in methylated neuroblastoma cell lines, whereas the expression of variant 2 was not. Variant 3, lacking a part of exon 5, was not expressed in neuroblastoma cell lines regardless of methylation status within CpG island and 5-aza-dCyd treatment. Those results suggested that the methylation of CpG residues in region 2 might be mainly responsible for the silencing of variant 1 of the *NR1I2* gene starting transcription from exon 1a in neuroblastoma, although region 2 does not contain its transcriptional start site.

Promoter activity of the CpG island located around exon 3 of *NR1I2*. Because the CpG island (region 2) of *NR1I2* was located around exon 3, we first determined whether region 2 had promoter activity by means of a luciferase reporter assay. This fragment alone (Fig. 2*A*, *2/L*) revealed clear promoter activity, whereas region 1 fragment upstream of exon 1 (Fig. 2*A*, *1/L*) showed almost none (Fig. 2*B*). In addition, we next determined whether region 2 acts as an enhancer to stimulate transcription from exon 1 by testing the luciferase activity in construct

[6] http://www.ncbi.nlm.nih.gov/.
[7] http://www.ncbi.nlm.nih.gov/IEB/Research/Acembly/index.html.

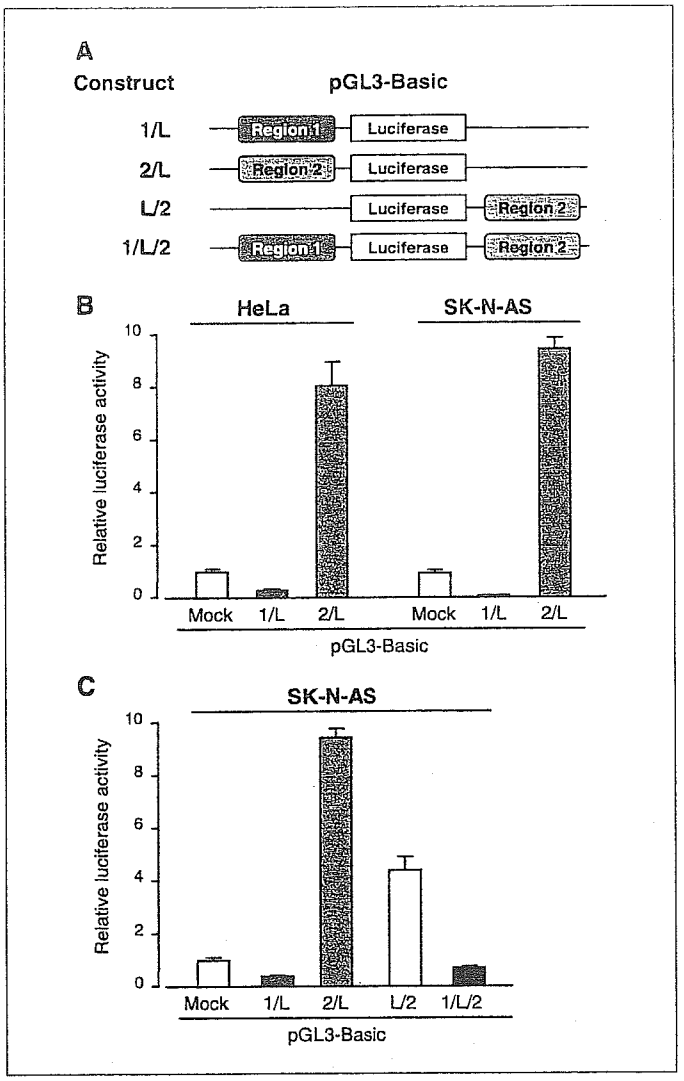

Figure 2. Promoter activity of the CpG island of *NR1I2*. pGL3-Basic vector, each containing a 1,060 bp 5′ fragment (region 1) or a 480 bp CpG island (region 2) of *NR1I2* in front of and/or downstream of the luciferase gene (*1/L*, *2/L*, *L/2*, and *1/L/2*; *A*), or pGL3-Basic empty vector (mock), was transfected into HeLa or SK-N-AS cells to evaluate promoter activity of region 1 and region 2 (*B*) and enhancer activity of region 2 (*C*). Luciferase activities were normalized versus an internal control. *Columns*, means of three separate experiments, each done in triplicate; *bars*, SE.

containing region 1 in front of the luciferase reporter gene and region 2 downstream of the luciferase gene (Fig. 2*A*, *1/L/2*). Although region 2 downstream of the luciferase gene (Fig. 2*A*, *L/2*) showed some promoter activity, region 2 revealed no enhancer activity for region 1 (Fig. 2*C*).

Analysis of *NR1I2* methylation and expression in primary neuroblastoma tumors. We next examined methylation status of the *NR1I2* CpG island in 51 surgically resected primary neuroblastomas using COBRA (Table 2). Clearly methylated alleles were detected in nine of the tumors (17%; Fig. 3*A*). The appearance of partial methylation observed in those nine tumors can be explained by the unavoidable contamination of non-tumorous cells in the specimens. Five of the nine tumors (55%) had undergone *MYCN* amplification, whereas only 3 of 42 (7%) unmethylated tumors showed amplification of *MYCN* (Table 2). Moreover, methylation of region 2 of the *NR1I2* gene was more frequently detected in advanced tumors (stages III and IVa; P = 0.0234, Fisher's exact test), tumors from patients with poor outcome (dead from disease; P = 0.0135, Fisher's exact test), and tumors from patients >1 year old (P = 0.052, Fisher's exact test), although the difference did not quite reach statistical significance in terms of patient age. In the 47 neuroblastoma cases where high-quality RNAs were available for expression analysis, a clear correlation between the methylation status of the CpG island and expression level of *NR1I2* mRNA was observed (Fig. 3*B* and *C*). By means of real-time quantitative RT-PCR experiments, we saw a statistically significant inverse correlation between expression of *NR1I2* mRNA and tumor stage (P = 0.0137, Mann-Whitney U test) or *MYCN* amplification (P = 0.0003, Mann-Whitney U test; Fig. 3*C*).

Suppression of cell growth after restoration of NR1I2 expression. To gain further insight into the potential role of NR1I2 in neuroblastoma carcinogenesis, we investigated whether restoration of NR1I2 expression would suppress growth of neuroblastoma cells lacking endogenous *NR1I2* expression using two *NR1I2* expression constructs, a Myc-tagged full coding sequence of *NR1I2* alone (pCMV-Tag3-*NR1I2*) and one fused to the constitutively active herpes virus VP-16 transactivation domain (pCMV-Tag3-*VP-NR1I2*). The VP-16-NR1I2 chimeric protein showed stronger transactivating activity than NR1I2 alone in a reporter assay using a reporter construct containing *NR1I2* response elements from the *CYP3A4* promoter (data not shown). After selecting drug-resistant colonies in transient transfection experiments, we found that colonies of *NR1I2*-transfected cells were remarkably fewer than in cultures of control transfectants and the effect of VP-16-NR1I2 was much greater than that of NR1I2 (Fig. 4*A*). Furthermore, VP-16-NR1I2 stable transfectants

Table 2. Correlation between patient profiles and *NR1I2* methylation status in 51 cases with neuroblastoma

Characteristics	Cases *n*	COBRA on *NR1I2* region 2*		
		Negative *n*	Positive *n*	*P*†
Total	51	42	9	
Age (y)				
<1	33	30	3	0.052
≥1	18	12	6	
Stage‡				
I, II, IVS	30	23	2	**0.0234**
III, IVa	21	16	7	
MYCN				
Nonamplified	43	39	4	**0.024**
Amplified	8	3	5	
Outcome				
Alive	44	39	5	**0.0135**
Dead	7	3	4	

NOTE: Statistically significant values are in boldface.
*COBRA was done as described in Materials and Methods.
†*P* values are from Fisher's exact test and were statistically significant when <0.05.
‡Tumor stage was classified according to the International Neuroblastoma Staging System.

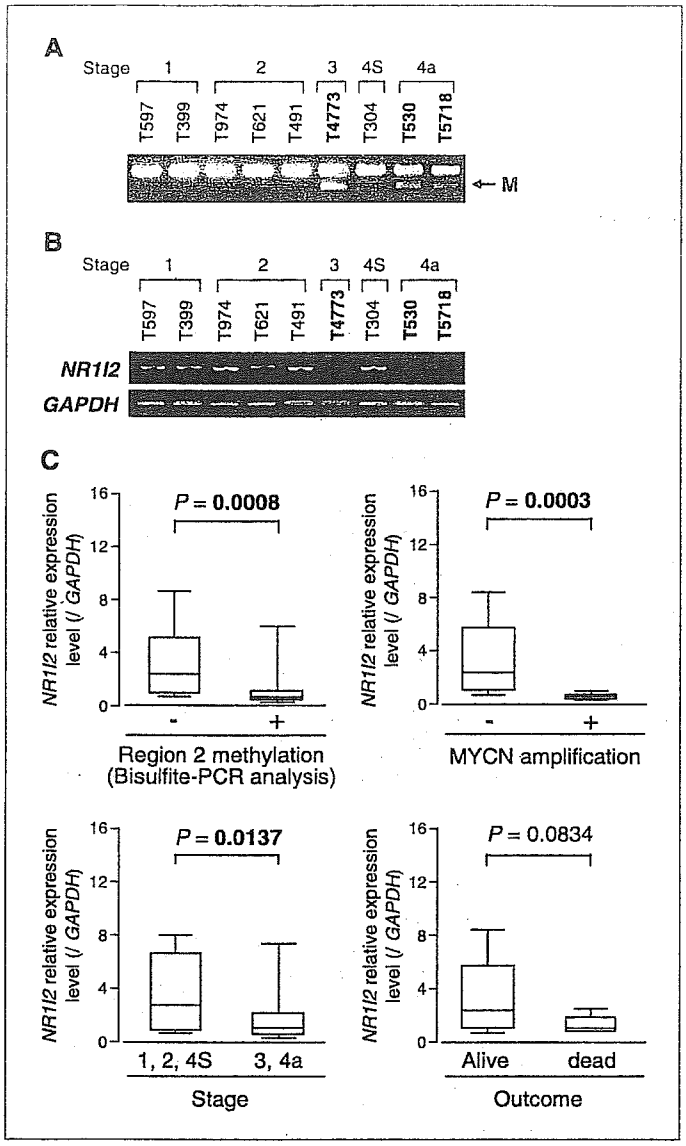

Figure 3. Methylation status and expression levels of *NR1I2* in primary neuroblastoma tumors. *A*, representative results of COBRA of the *NR1I2* CpG island (region 2). *M*, methylated alleles restricted by *Hha*I. *B*, representative results of RT-PCR analysis of *NR1I2* mRNA expression. *GAPDH* was used as an internal control. Note that tumors showing methylation in Fig. 2*A* (T4773, T530, and T5718) showed decreased expression of *NR1I2*. *C*, expression of *NR1I2* mRNA in primary neuroblastoma tumors, compared with methylation status of the CpG island of *NR1I2* region 2, *MYCN* amplification status, tumor stage, and patient outcomes. The levels of *NR1I2* mRNA expression were determined by real-time quantitative RT-PCR experiments. Significantly higher expression of *NR1I2* was observed in tumors without methylation of the CpG island ($P = 0.0008$; Mann-Whitney *U* test), in stage I, II, and IVS tumors ($P = 0.0137$, Mann-Whitney *U* test), and in *MYCN*-nonamplified tumors ($P = 0.0003$, Mann-Whitney *U* test) compared with tumors with methylation of the CpG island, stage III or IVa tumors, and *MYCN*-amplified tumors. Higher expression of *NR1I2* was also observed in living, disease-free patients compared with those who had died of their tumors, although the difference did not reach statistical significance ($P = 0.0834$, Mann-Whitney *U* test).

established from a cell line (SMS-KAN) without endogenous expression of this gene showed a lower growth rate than control vector-transfected cells regardless of VP-16-NR1I2 expression level (Fig. 4*B* and *C*). The same result was obtained in other cell line (data not shown).

Screening of possible target genes for NR1I2. To identify possible transcriptional targets for NR1I2, we did expression array analysis in an independent VP-16-NR1I2 stable transfectant established from SMS-KAN, in a comparison with vector-transfected cells. We twice obtained independent experimental data (first, Cy3-B1/Cy5-vector; second, Cy5-B1/Cy3-vector) and compiled a list of 105 genes that showed ratios >1.5 in both experiments (Supplementary Table S1). Semiquantitative RT-PCR analysis revealed up-regulation of *CYP3A4*, a known transcriptional target of *NR1I2*, in VP-16-NR1I2 stable transfectant, indicating the reliability of our system for detecting target genes (Supplementary Fig. S1). To validate the expression array data, we did semiquantitative RT-PCR analyses of 10 other genes (Fig. 4*D*), which have been previously reported as tumor-associated genes, using two independent VP-16-NR1I2 stable transfectants established from SMS-KAN cells (KAN-B1 and KAN-B2) and one stable transfectant from GOTO cells (GOTO-A1). GOTO-A1 also showed a lower growth rate than control vector-transfected cells (data not shown). The RT-PCR results for KAN-B1 confirmed up-regulation of seven genes except for *BARD1*, *EXT1*, and *MCM5* (Fig. 4*D*). Notably, only *PLA2G2A* showed increased expression in all stable transfectants examined compared with their control cells (Fig. 4*D*; Supplementary Fig. S1).

Discussion

In the study presented here, we identified a novel target for CpG island methylation, *NR1I2*, observed mainly in advanced neuroblastomas, through a genome-wide exploration of highly methylated DNA fragments using BAMCA. A clear inverse correlation emerged between CpG island methylation and the expression status of *NR1I2* both in cell lines and primary tumors of neuroblastoma (i.e., hypermethylation and silencing of *NR1I2* were more frequent in advanced neuroblastoma tumors). Together with a shown growth suppressive effect of exogenous NR1I2, the data suggested that *NR1I2* was likely to be a tumor suppressor gene associated with clinical and/or biological aggressiveness of neuroblastoma. Our results further underscored the promise of BAMCA as a high-throughput screening method for methylated sites in cancer genomes on an array platform.

BAMCA, however, has some disadvantages: (*a*) It examines only a limited number of CpG sites within a CpG island because only *Sma*I/*Xma*I sites are used to search differentially methylated CpGs. (*b*) It identifies BACs, which contain differentially methylated sequences between test and reference DNAs, although sequences are not always associated with promoter regions of genes. (*c*) It misses differentially methylated sequences/genes without BACs spotted on the BAC array used. To improve the sensitivity of array-based methylation screening, it is possible to use other methylation-sensitive restriction sites as indicators, including *Not*I site (20). However, BAMCA may quickly provide the list of possible target genes for methylation within identified BAC clones using information from human genome database without cloning and sequencing of enriched fragments, suggesting that it may have important applications in population-based studies of CpG island methylation.

NR1I2 locates at 3q13.33, a chromosomal region that is not often involved in loss of heterozygosity or copy number losses in neuroblastoma (21, 22). Indeed, most of the cell lines we used in this study showed normal copy number in 3q (13), suggesting that a homozygous inactivation of *NR1I2* might occur by biallelic

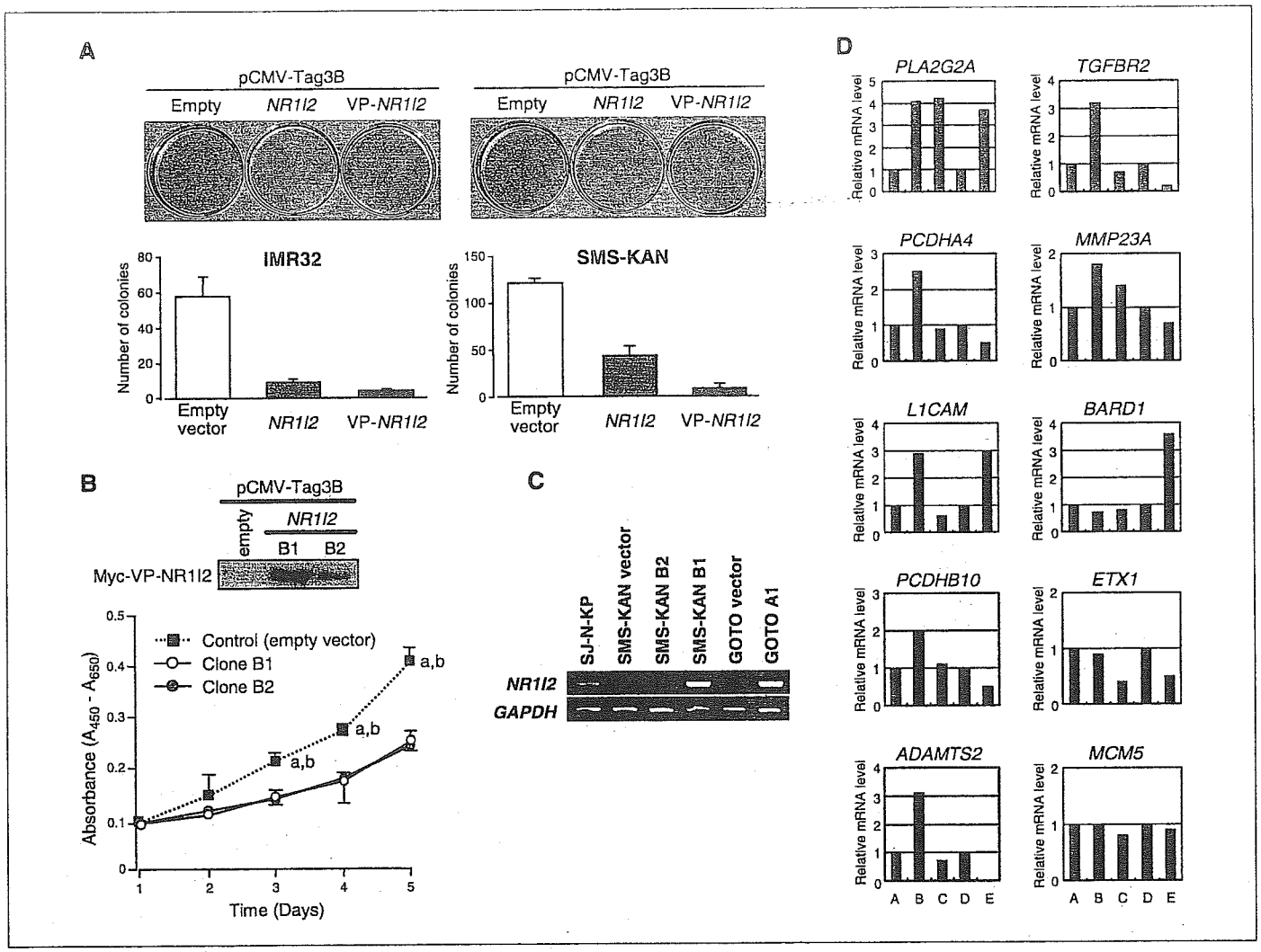

Figure 4. Effect of restoration of NR1I2 expression on growth of neuroblastoma cells. *A, top,* colony formation assays using neuroblastoma cell lines. Cells without *NR1I2* expression (IMR32 and SMS-KAN) were transfected with Myc-tagged construct containing *NR1I2* (pCMV-Tag3B-*NR1I2*), *VP-NR1I2* (pCMV-Tag3B-*VP-NR1I2*), or empty vector (pCMV-Tag3B), and selected for 3 weeks with G418. *Bottom,* quantitative analysis. *Columns,* mean of three separate experiments, each done in triplicate; *bars,* SE. *B,* inhibitory effect of stably transfected *NR1I2* on the growth of SMS-KAN cells transfected with pCMV-Tag3B-*VP-NR1I2* or empty vector and selected with G418 to establish clones stably expressing NR1I2. *Top,* two clones transfected with pCMV-Tag3B-*VP-NR1I2* (B1 and B2) were subjected to Western blot analysis using 10 μg of protein extract and anti-Myc-Tag antibody. Both expressed Myc-tagged VP-NR1I2 protein. *Bottom,* effect of stable NR1I2 expression on the growth of SMS-KAN cells. Cell viability was determined by water-soluble tetrazolium salt assay at the indicated times. *Points,* means of three separate experiments; *bars,* SE. Statistical analysis used the Mann-Whitney *U* test: *a,* control versus clone B1; *b,* control versus clone B2. All $P < 0.05$. *C,* the mRNA expression level of *NR1I2* in endogenously NR1I2-positive cells (SK-N-KP) as well as stably transfected cells (SMS-KAN-B1, SMS-KAN-B2, and GOTO-A1) and their mock-transfected control (KAN-vector and GOTO-vector). *D,* confirmation of microarray results by semiquantitative RT-PCR of possible target genes using two stable transfectants established from SMS-KAN (KAN-B1 and KAN-B2) and one transfectant from GOTO (GOTO-A1) with their mock-transfected control cells *A,* SMS-KAN mock-control; *B,* KAN-B1; *C,* KAN-B2; *D,* GOTO mock-control; *E,* GOTO-A1. PCR products were electrophoresed in 3% agarose gel and band quantification was done with LAS-3000 (Fujifilm, Tokyo, Japan). After normalization with *GAPDH*, expression level of each gene in each transfectant relative to its corresponding mock-transfected control was recorded as a fold increase in relative expression level. Primer sequences and cycling numbers for PCR of each gene are available on request.

methylation. Similar findings have been reported for several genes, such as *RASSF1* (3p21.3), *DAPK* (9q34.1), and *THBS1* (15q15), which are located in regions not frequently deleted, although some methylated genes, such as *ARF* and *INK4A* (9p21), and *CASP8* (2q23), are in fact on regions frequently deleted in neuroblastoma (23). Therefore, both biallelic methylation and monoallelic methylation with allele loss may be important mechanisms for inactivating tumor-associated genes in this disease.

Our promoter assays showed that CpG island around exon 3 (region 2) shows promoter activity, but CpG-rich 5′ region containing exon 1 and its 5′ upstream sequences (region 1) does not. Region 2 shows no enhancer activity for region 1 (Fig. 2). The methylation status of region 2, but not region 1, was highly and inversely correlated with the expression of *NR1I2*, especially the most major variant of *NR1I2*, variant 1, starting from exon 1a. Those results suggest that the methylation status of CpG residues in region 2 might be responsible for the silencing of this gene and contributed to loss of function of NR1I2 protein in neuroblastoma. A few studies, including ours, have shown that promoter activity can occur in fragments, especially CpG islands, not containing transcriptional starting sites (17, 24, 25). It is possible that methylation that occurred in those CpG islands with promoter activity may silence gene expression from specific starting sites.

Among numerous hypermethylated genes reported in neuroblastoma (3–8), *CASP8* seems to be inactivated through promoter methylation in advanced neuroblastoma tumors where *MYCN* is amplified (4). Those findings, along with ours, suggest that (*a*) unknown mechanisms contribute to progression of neuroblastoma by causing genetic alterations, including *MYCN* amplification, as well as methylation-mediated inactivation of a subset of tumor suppressor genes; (*b*) methylation-mediated inactivation of a subset of tumor suppressor genes may cause genetic changes that lead to progression of neuroblastoma; or (*c*) *MYCN* amplification and/or other alterations in advanced neuroblastomas may bring about a CpG island methylator phenotype (3). Gonzalez-Gomez et al. (23) reported that higher aggressiveness, represented at the molecular level by concurrent *MYCN* amplification and 1p loss in neuroblastoma, was not paralleled by an accumulation of methylation events among various genes they examined, suggesting that CpG island methylation in advanced neuroblastoma could be specific to a subset of genes.

The *NR1I2* gene encodes an orphan nuclear receptor that plays a key role in the regulation of xenobiotic response by controlling expression of drug metabolizing and clearance molecules (26–28). NR1I2 protein activates expression of genes encoding proteins such as CYP3A4 and ABCB1, which reduce the concentrations of xenochemicals and toxic bile acids (29). However, effects of NR1I2 on cell growth or expression of growth-regulating genes have never been clarified, although we have shown here that the induction of ectopic NR1I2 inhibited growth of neuroblastoma cells. Other nonsteroidal nuclear receptors, such as all-*trans* retinoic acid receptor and vitamin D_3 receptor, which form heterodimers with the 9-*cis* retinoic acid receptor in the same way as NR1I2, mediate antiproliferative and differentiation-promoting activities toward several malignant cell types (30, 31). Therefore, growth-suppressive activity might be one of the normal functions of NR1I2 although its mechanisms remain unknown.

To achieve some clarity with respect to the growth inhibitory activity of NR1I2, we tried to determine its putative transcriptional targets. Among 105 genes through an expression array analysis, we selected 10 genes for validation by semiquantitative PCR based on their possible cancer-associated function (Online Mendelian Inheritance in Man),[8] and identified one candidate, *PLA2G2A*, encodes secretory phospholipase A2, as a possible target of NR1I2, although it will be needed to determine whether *PLA2G2A* is a direct or indirect target. This product qualifies as a tumor suppressor because mice lacking *PLA2G2A* expression show increased colonic polyposis (32). Interestingly, *PLA2G2A* was mapped to chromosome 1p36, a region frequently implicated in the pathogenesis of neuroblastoma (33). Further screening of possible targets of NR1I2 will be necessary to clarify how NR1I2 regulates neuroblastoma cell growth.

Because only 7 of 51 neuroblastoma patients in our study died during follow-up periods, we did not perform a survival analysis. However, the high prevalence of *NR1I2* silencing through DNA methylation that we observed in aggressive neuroblastomas, along with the shown growth suppression activity of NR1I2, indicate that this molecule might serve as a diagnostic marker to predict prognosis.

Acknowledgments

Received 3/30/2005; revised 9/2/2005; accepted 9/13/2005.

Grant support: Grants-in-Aid for Scientific Research on Priority Areas (C) from the Ministry of Education, Culture, Sports, Science, and Technology, Japan; a Grant-in-Aid from Core Research for Evolutionary Science and Technology of Japan Science and Technology; Center of Excellence program for Frontier Research on Molecular Destruction and Reconstitution of Tooth and Bone; program for promotion of Fundamental Studies in Health Sciences of the Pharmaceuticals and Medical Devices Agency; and Third Term Comprehensive Control Research for Cancer of the Ministry of Health, Labour, and Welfare.

The costs of publication of this article were defrayed in part by the payment of page charges. This article must therefore be hereby marked *advertisement* in accordance with 18 U.S.C. Section 1734 solely to indicate this fact.

We thank Ai Watanabe and Ayako Takahashi for technical assistance.

[8] http://www.ncbi.nlm.nih.gov/Omim/omimhelp.html.

References

1. Brodeur GM. Neuroblastoma: biological insights into a clinical enigma. Nat Rev Cancer 2003;3:203–16.
2. Westermann F, Schwab M. Genetic parameters of neuroblastomas. Cancer Lett 2002;184:127–47.
3. Abe M, Ohira M, Kaneda A, et al. CpG island methylator phenotype is a strong determinant of poor prognosis in neuroblastomas. Cancer Res 2005;65:828–34.
4. Teitz T, Wei T, Valentine MB, et al. Caspase 8 is deleted or silenced preferentially in childhood neuroblastomas with amplification of MYCN. Nat Med 2000;6:529–35.
5. Astuti D, Agathanggelou A, Honorio S, et al. RASSF1A promoter region CpG island hypermethylation in phaeochromocytomas and neuroblastoma tumours. Oncogene 2001;20:7573–7.
6. Yan P, Muhlethaler A, Bourloud KB, Beck MN, Gross N. Hypermethylation-mediated regulation of CD44 gene expression in human neuroblastoma. Genes Chromosomes Cancer 2003;36:129–38.
7. Yang Q, Liu S, Tian Y, et al. Methylation-associated silencing of the thrombospondin-1 gene in human neuroblastoma. Cancer Res 2003;63:6299–310.
8. Yang Q, Liu S, Tian Y, et al. Methylation-associated silencing of the heat shock protein 47 gene in human neuroblastoma. Cancer Res 2004;64:4531–8.
9. Baylin SB, Herman JG, Graff JR, Vertino PM, Issa JP. Alterations in DNA methylation: a fundamental aspect of neoplasia. Adv Cancer Res 1998;72:141–96.
10. Ushijima T. Detection and interpretation of altered methylation patterns in cancer cells. Nat Rev Cancer 2005;5:223–31.
11. Toyota M, Ho C, Ahuja N, et al. Identification of differentially methylated sequences in colorectal cancer by methylated CpG island amplification. Cancer Res 1999;59:2307–12.
12. Inazawa J, Inoue J, Imoto I. Comparative genomic hybridization (CGH)-arrays pave the way for identification of novel cancer-related genes. Cancer Sci 2004;95:559–63.
13. Saito-Ohara F, Imoto I, Inoue J, et al. PPM1D is a potential target for 17q gain in neuroblastoma. Cancer Res 2003;63:1876–83.
14. Brodeur GM, Pritchard J, Berthold F, et al. Revision of the international criteria for neuroblastoma diagnosis, staging, and response to treatment. J Clin Oncol 1993;11:1466–77.
15. Matsumura T, Michon J. Treatment of localized neuroblastoma. In: Brodeur GM, Sawada T, Tsuchida Y, Voute PA, editors. Neuroblastoma. Amsterdam (the Netherlands): Elsevier Science BV; 2000. p. 403–16.
16. Tsuchida Y, Kaneko M. Treatment of advanced neuroblastoma: the Japanese experience. In: Brodeur GM, Sawada T, Tsuchida Y, Voute PA, editors. Neuroblastoma. Amsterdam (the Netherlands): Elsevier Science BV; 2000. p. 453–70.
17. Sonoda I, Imoto I, Inoue J, et al. Frequent silencing of low density lipoprotein receptor-related protein 1B (LRP1B) expression by genetic and epigenetic mechanisms in esophageal squamous cell carcinoma. Cancer Res 2004;64:3741–7.
18. Inoue J, Otsuki T, Hirasawa A, et al. Overexpression of PDZK1 within the 1q12-q22 amplicon is likely to be associated with drug-resistance phenotype in multiple myeloma. Am J Pathol 2004;165:71–81.
19. Lamba V, Yasuda K, Lamba JK, et. al. PXR (NR1I2): splice variants in human tissues, including brain, and identification of neurosteroids and nicotine as PXR activators. Toxicol Appl Pharmacol 2004;199:251–65.
20. Ching TT, Maunakea AK, Jun P, et al. Epigenome analyses using BAC microarrays identify evolutionary conservation of tissue-specific methylation of *SHANK3*. Nat Genet 2005;37:645–51.
21. Brinkschmidt C, Christiansen H, Terpe HJ, et al. Comparative genomic hybridization (CGH) analysis of neuroblastomas—an important methodological approach in paediatric tumour pathology. J Pathol 1997;181:394–400.
22. Takita J, Hayashi Y, Yokota J. Loss of heterozygosity in neuroblastomas—an overview. Eur J Cancer 1997;33:1971–3.
23. Gonzalez-Gomez P, Bello MJ, Lomas J, et al. Aberrant methylation of multiple genes in neuroblastic tumours. Relationship with MYCN amplification and allelic status at 1p. Eur J Cancer 2003;39:1478–85.
24. Kolb A. The first intron of the murine β-casein gene contains a functional promoter. Biochem Biophys Res Commun 2003;306:1099–105.

25. Nakagawachi T, Soejima H, Urano T, et al. Silencing effect of CpG island hypermethylation and histone modifications on *O6*-methylguanine-DNA methyltransferase (MGMT) gene expression in human cancer. Oncogene 2003;22:8835–44.
26. Blumberg B, Sabbagh W, Juguilon H, et al. SXR, a novel steroid and xenobiotic-sensing nuclear receptor. Genes Dev 1998;12:3195–205.
27. Kliewer SA, Moore JT, Wade L, et al. An orphan nuclear receptor activated by pregnanes defines a novel steroid signaling pathway. Cell 1998;92:73–82.
28. Xie W, Barwick JL, Downes M, et al. Humanized xenobiotic response in mice expressing nuclear receptor SXR. Nature 2000;406:435–9.
29. Synold TW, Dussault I, Forman BM. The orphan nuclear SXR coordinately regulates drug metabolism and efflux. Nat Med 2001;7:584–90.
30. Altucci L, Gronemeyer H. Nuclear receptors in cell life and death. Trends Endocrinol Metab 2001;12:460–8.
31. Rao A, Coan A, Welsh JE, Barclay WW, Koumenis C, Cramer SD. Vitamin D receptor and p21/WAF1 are targets of genistein and 1,25-dihydroxyvitamin D_3 in human prostate cancer cells. Cancer Res 2004;64:2143–7.
32. Haluska FG, Thiele C, Goldstein A, Tsao H, Benoit EP, Housman D. Lack of phospholipase A2 mutations in neuroblastoma, melanoma and colon-cancer cell lines. Int J Cancer 1997;72:337–9.
33. Praml C, Savelyeva L, Le Paslier D, et al. Human homologue of a candidate for the Mom1 locus, the secretory type II phospholipase A2 (PLA2S-II), maps to 1p35–36.1/D1S199. Cancer Res 1995;55:5504–6.

Available online at www.sciencedirect.com
SCIENCE DIRECT
ELSEVIER
Cancer Letters 228 (2005) 267–270
CANCER Letters
www.elsevier.com/locate/canlet

Diversity in neuroblastomas and discrimination of the risk to progress

Takeo Tanaka[a,*], Tomoko Iehara[b], Tohru Sugimoto[b], Minoru Hamasaki[c], Satoshi Teramukai[d], Yoshiaki Tsuchida[e], Michio Kaneko[e], Tadashi Sawada[b,d]

[a]*Department of Pediatrics and Division of Clinical Research, National Hospital Organization, Kure Medical Center, Hiroshima, Japan*
[b]*Department of Pediatrics, Kyoto Prefectural University of Medicine, Kyoto, Japan*
[c]*Department of Pathology, Shizuoka Children's Hospital, Shizuoka, Japan*
[d]*The Japanese Infantile Neuroblastoma Cooperative Study*
[e]*The Japanese Advanced Neuroblastoma Cooperative Study*

Received 26 November 2004; accepted 2 December 2004

Abstract

The clinical diversity of Neuroblastomas (NBs) was discriminated into three groups with high sensitivity and specificity to patient's outcome. The '*high risk*' NB is defined with any of following conditions, MYCN amplification or unfavorable histology of International Neuroblastoma Pathological Classification (INPC) or low Ha-ras/trk A expression. The '*low risk*' NB is defined with all following conditions, single copy of MYCN and INPC favorable histology and high Ha-ras/trk A expression and localized tumor. The remaining NBs were classified into '*intermediate risk*' ones. According to these criteria, the diversity of the 248 mass-screening NBs was shown with variety progressive risk; 40% were classified in *low risk group*, 25% were in *high risk group* and 35% were in *intermediate risk group*.

Keywords: Neuroblastoma; Risk discrimination; *MYCN*; INPC; Ha-ras; Trk A; Mass-screening.

1. Introduction

Neuroblastoma (NB) is the most common extracranial solid malignancy in childhood. This malignancy shows diversity in their clinical behavior. Recent advances in molecular and genetic approach promote to understand their biology and provide predictors associated with clinical behavior of NBs [1]. MYCN amplification is a powerful predictor with high specificity to aggressiveness of NBs [2], however, the sensitivity is only a half of the patients with poor clinical outcome [3]. Brodeur [4] proposed three types of NBs classified according to several biological markers. The clinical evaluation whether we can get predictive specificity and sensitivity enough to use for the patients has not been done yet.

* Corresponding author. Tel.: +81 823 22 3111; fax: +81 823 22 0478.
E-mail address: ttanaka@kure-nh.go.jp (T. Tanaka).

0304-3835/$ - see front matter © 2005 Elsevier Ireland Ltd. All rights reserved.
doi:10.1016/j.canlet.2004.12.051